# Accepted Manuscript


Synthesis, and evaluation of *in vitro* and *in vivo* anticancer activity of 14-substituted oridonin analogs: A novel and potent cell cycle arrest and apoptosis inducer through the p53-MDM2 pathway

Qing-Kun Shen, Hao Deng, Shi-Ben Wang, Yu-Shun Tian, Zhen-Shan Quan

PII: S0223-5234(19)30304-6

DOI: https://doi.org/10.1016/j.ejmech.2019.04.005

Reference: EJMECH 11240

To appear in: *European Journal of Medicinal Chemistry*

Received Date: 25 December 2018

Revised Date: 1 April 2019

Accepted Date: 1 April 2019

Please cite this article as: Q.-K. Shen, H. Deng, S.-B. Wang, Y.-S. Tian, Z.-S. Quan, Synthesis, and evaluation of *in vitro* and *in vivo* anticancer activity of 14-substituted oridonin analogs: A novel and potent cell cycle arrest and apoptosis inducer through the p53-MDM2 pathway, *European Journal of Medicinal Chemistry* (2019), doi: https://doi.org/10.1016/j.ejmech.2019.04.005.

# Synthesis, and evaluation of in *vitro* and in *vivo* anticancer activity of 14-substituted oridonins: A novel and potent cell cycle arrest and apoptosis inducers through the p53-MDM2 pathway

Qing-Kun Shen[1], Hao-Deng[1], Shi-Ben Wang[2], Hao Deng[1], Yu-Shun Tian[1]* and Zhen-Shan Quan[1]*

[1]*Key Laboratory of Natural Resources and Functional Molecules of the Changbai Mountain, Affiliated Ministry of Education, College of Pharmacy, Yanbian University, Yanji, Jilin, 133002, China*

[2]*School of Pharmacy, Liaocheng University, LiaoCheng, Shandong, 252059, China*

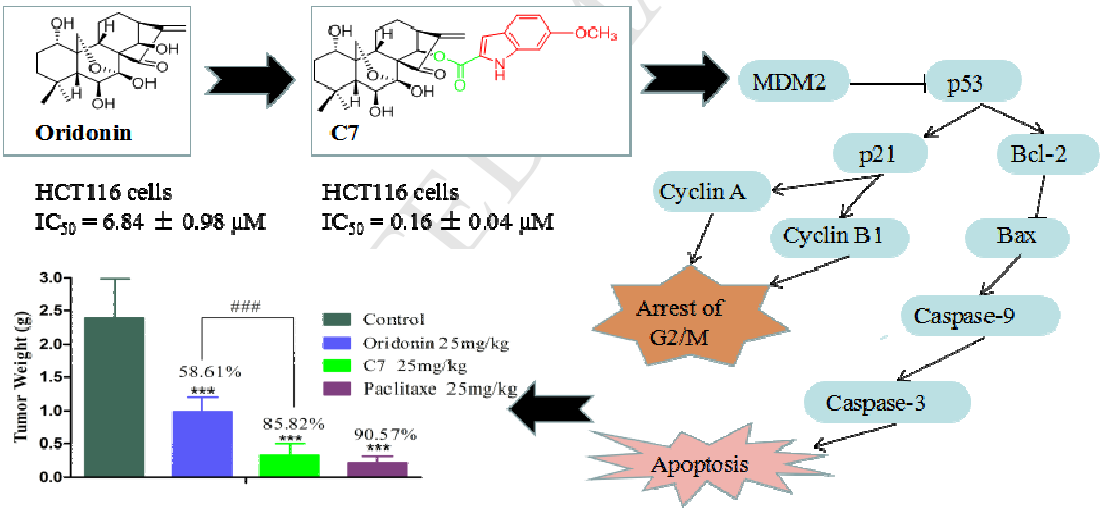

# Synthesis, and evaluation of *in vitro* and *in vivo* anticancer activity of 14-substituted oridonin analogs: A novel and potent cell cycle arrest and apoptosis inducer through the p53-MDM2 pathway

Qing-Kun Shen[1$], Hao-Deng[1$], Shi-Ben Wang[2], Yu-Shun Tian[1]* and Zhen-Shan Quan[1]*

[1]*Key Laboratory of Natural Resources and Functional Molecules of the Changbai Mountain, Affiliated Ministry of Education, College of Pharmacy, Yanbian University, Yanji, Jilin, 133002, China*

[2]*School of Pharmacy, Liaocheng University, LiaoCheng, Shandong, 252059, China*

***Corresponding author: Tel: + 86 433 243-6004; Fax: + 86 433 243-6004.**

**E-mail: ystian@ybu.edu.cn (Y. S. Tian).**

***Corresponding author: Tel: + 86 433 243-6020; Fax: + 86 433 243-6020.**

**E-mail: zsquan@ybu.edu.cn (Z. S. Quan).**

[$]These authors contributed equally

**Abstract**

A series of novel oridonin derivatives bearing various substituents on the 14-OH position were designed and synthesised. Their antitumour activity was evaluated *in vitro* against three human cancer cell lines (HCT116, BEL7402, and MCF7). Most tested derivatives showed improved anti-proliferative activity compared to the lead compound oridonin and the positive control drug 5-fluorouracil (5-Fu). Among them, compound **C7** ($IC_{50}$ = 0.16 $\mu$M) exhibited the most potent anti-proliferative activity against HCT116 cells; it was about 43- and 155-fold more efficacious than that of oridonin ($IC_{50}$ = 6.84 $\mu$M) and 5-Fu ($IC_{50}$ = 24.80 $\mu$M) in HCT116 cancer cells. Interestingly, the $IC_{50}$ value of compound **C7** in L02 normal cells was 23.6-fold higher than that in HCT116 cells; it exhibited better selective anti-proliferative activity and specificity than oridonin and 5-Fu. Furthermore, compound **C7** possibly induced cell cycle arrest and apoptosis by regulating the p53-MDM2 signalling pathway. Notably, **C7** displayed more significant suppression of tumour growth than oridonin in colon tumour xenograft models where the tumour growth inhibition rate was 85.82%. Therefore, compound **C7** could be a potential lead compound for the development of a novel antitumour agent.

**Key words:** Oridonin; Antitumour; ; Apoptosis; Cell cycle arrest; *In vivo*

## 1. Introduction

Recently, malignant tumours have become a serious health issue as their incidence has been increasing yearly [1]. So far, drug therapy is still an effective and important method in the clinical treatment of cancer. One of the major obstacles to the druggability of compounds with effective antitumour activity is their toxicity to normal cells. Therefore, the development of novel anticancer agents with lower toxicity to normal cells is needed. Natural products play a leading role in drug discovery. About 65% of the 1211 drugs and small-molecule new chemical entities approved for marketing in 1981-2014 are directly or indirectly derived from natural products [2]. Thus, structural modifications of active natural products is an effective way for discovering potentially active molecules, lead compounds, and new drugs.

Oridonin (Figure 1A), initially isolated from various Isodon species which are commonly used as a home remedy herb in China and Japan, was proven to possess a wide variety of pharmacological activities, such as antifibrosis [3-5], anticancer effects [6-7]. In the past few years, a number of oridonin derivatives have been designed and synthesised to yield better drug candidates with enhanced activities [8-19]. The analysis of the reported derivatives provided a clear structure activity relationship. Briefly, $\alpha$, $\beta$-unsaturated ketone is the active moiety of oridonin, and reduction or opening of this moiety will significantly reduce the anti-proliferative efficacy of oridonin [20-21]. Most derivatives with C-14 hydroxyl functional groups exhibit improved anti-proliferative activity. For instance, compound **J** (Figure 1A), oridonin-coupled nitrogen mustard conjugate at the C-14 hydroxyl, displayed improved anti-proliferative activity *in vitro* ($IC_{50}$ = 0.50 μM for BEL7402 cells), which was 15-fold more potent than that of oridonin [8]. Similarly, Xu *et al.* prepared a series of oridonin derivatives of a saturated, long-chain terminal acid in the C-14 position. Among them, compound **K** (Figure 1A) was identified as the most potent analogue of this series with an enhanced anti-proliferative effect ($IC_{50}$ = 2.06 $\mu$M against BEL7402 cells) compared to oridonin ($IC_{50}$ = 29.80 $\mu$M) [11]. In addition, compound HAO472 (Figure 1A), an L-alanine-(14-oridonin) ester trifluoroacetate, has been discovered and developed by Hengrui Medicine Co. Ltd in China for the

treatment of acute myelogenous leukaemia and it is now in Phase I of human clinical trials (CTR20150246; www.chinadrugtrials.org.cn) [22]. According to the examples illustrated in Figure 1A, it was rational to introduce active groups at the C-14 hydroxyl group of the $\alpha$, $\beta$-unsaturated ketone structure of oridonin.

Phenyl 1,2,3-triazole has a high dipole moment and can form a hydrogen bond with drugs target, which is beneficial for the binding of the compound to the target [23]. Thus, it is an important heterocyclic structural unit distributed in a large number of biologically active molecules as anti-bacterial [24-25], anti-malarial [26], anti-tubercular [27], anti-inflammatory [28-29], and anticancer molecules [30]. In recent years, natural active products and the phenyl 1, 2, 3 triazole molecular fragment were combined to improve the antitumour activity, physicochemical properties, and drug-forming properties of the natural products. The modification strategy of natural products such as compounds **L**, **M**, **N**, **O** and **P** in Figure 1B has attracted more attention [31-34]. Compound **N** is a synthetic xanthotoxin derivative designed according to a strategy described in our previous studies, which exhibited antitumour activity and low toxicity [32]. In particular, Zhou *et al.* utilized click reaction to generate a series of oridonin-based 1,2,3-triazole derivatives by introducing 1,2,3-triazoles into the C-1, C-2, or C-3 position of the A ring of oridonin. Among them, the representative triazole-substituted oridonin analogue **P** exhibits a 61-fold increase in antiproliferative potency ($EC_{50}$ = 0.48 $\mu$M) against the MDA-MB-231 triple-negative breast cancer cell line relative to oridonin ($EC_{50}$ = 29.4 $\mu$M)[34]. Therefore, a combination of 1,2,3-triazole groups with oridonin is an effective strategy to enhance its antitumour activity.

Indole is a bicyclic heterocycle, which widely distributed in natural products such as alkaloids, plants, animals, and microbial hormones [35,36]. As a special active fragment, indole has become the focus of attention in drug discovery and development [37]. Indole containing compounds showed anti-inflammatory [38,39], antiviral [40], antioxidant [41,42], and anticancer activities [43-45]. Interestingly, the molecular hybridisation of many natural products and indole significantly enhances their anticancer activity such as compounds **Q**, **R**, and **S** in Figure 1C [46-48].

Therefore, the introduction of indole active fragments in natural products is an effective modification strategy.

In this study, we selected oridonin as a lead compound and successfully introduced phenyl 1,2,3-triazoles and various indoles at the C-14 hydroxyl group of oridonin. Consequently, we designed and synthesised oridonin derivatives containing different phenyl 1, 2, 3-triazoles (**A1-9)**. In order to complete the structure activity relationship (SAR) study, we changed the linker between the two parts and designed and synthesised the target compounds **B1-B3**. Moreover, we designed and synthesised the oridonin derivatives **C1-C9** and **D1-D2** containing different substituted indoles. Compounds **E** and **F** have been designed and synthesised according to the alternative design of quinoline ring or isoquinoline ring because of their similar physicochemical and biological properties to the indole ring (Figure 2). Subsequently, all the 25 new compounds were screened against three different types of cancer cell lines. The toxicity of potential compounds in normal human liver L02 cells was also tested. In addition, the *in vivo* antitumour efficacy and mechanism of action of the most promising compound **C7** was also investigated.

## 2. Results and discussion

### *2.1 Chemistry*

Preparation of the intermediates is shown in Scheme 1. Compounds **1a-1i** was obtained by diazotisation and azide reactions of various anilines [49]. Then, a click reaction between intermediates **1a-1i** and propionic acid or propylamine gave compounds **2a-2i** and compound **3a-3c**, respectively with good yields [50]. Compounds **3a-3c** was mixed with succinic anhydride in $CH_2Cl_2$ at room temperature to give compounds **4a-4c**. Commercially available 4-substituted anilines were replaced by hydrazine, reacted with pyruvic acid, cyclised, and then hydrolysed with NaOH to obtain different 5-substituted indole-2-acids **8a-8c**. Simultaneously, other substituted indole-2-acid intermediates **8d-8i** were obtained by condensation of different substituted benzaldehydes with ethyl-2-azidoacetate followed by cyclisation and hydrolysation of NaOH [51]. Indole-3-carboxylic acid mixed with $CH_3I$ and

catalysed by KOH in dimethylformamide (DMF) at room temperature produced compound **9**. When indole-3-carboxylic acid was mixed with di-tert-butyl dicarbonate and catalysed by 4-dimethylaminopyridine (DMAP) in $CH_2Cl_2$ at room temperature, it produced compound **10** [52,53].

The general path to synthesise the target oridonin analogues **A1-A9**, **B1-B3**, **C1-C9**, **D1**,**D3**, **E**, and **F** is shown in Scheme 2. Oridonin as a starting material and target compounds **A1-A9** and **B1-B3** were obtained by an amide condensation reaction with different acid catalysed by 1-(3-dimethylaminopropyl)-3-ethylcarbodiimide hydrochloride (EDCI) and DMAP in anhydrous $CH_2Cl_2$ at 0□; under these conditions, only the C-14 hydroxyl group is condensed with different carboxylic acids [54-55]. All the synthesised compounds were characterised by $^{1}$H NMR, $^{13}$C NMR, and HRMS approaches.

*2.2. Biological evaluation*

*2.2.1. In vitro anti-proliferative activity and SAR study*

The anti-proliferative activities against three human cancer cell lines including HCT116 (human colorectal cancer cell line), MCF-7 (human breast cancer cell line), and BEL7402 (human hepatocellular carcinoma cell line), were established for all the target compounds by the MTT assay. The $IC_{50}$ values (concentration required to inhibit tumour cell proliferation by 50%) are listed in Table 1; oridonin and 5-Fu are used as positive controls. As shown in Table 1, all oridonin derivatives **A1**-**A9** containing different phenyl 1,2,3-triazoles exhibited stronger anti-proliferative activities against all three selected cancer cell lines than oridonin and 5-Fu. Among them, compound **A6** with 4-methoxyphenyl 1,2,3-triazole, was the most potent compound in this series with an $IC_{50}$ value of 1.94 $\mu$M in HCT116 cell line. It was about 3-fold more potent than oridonin in the cancer cell lines tested. Compound **A5** containing 4-methylphenyl 1,2,3-triazole was the most potent compound in this series, with an $IC_{50}$ value of 3.01 $\mu$M in MCF-7 cell lines. It was about 6-fold more potent than oridonin in the cancer cell lines tested. In order to explore the effect of the linker on the anti-proliferative activity between oridonin and 1,2,3-triazole, we designed and

synthesised compounds **B1-B3** with methyl 4-(methylamino)-4-oxobutanoate instead of ester. Interestingly, these compounds do not further enhance anti-proliferative activity, exhibiting only similar activities as that of the lead compound oridonin, which indicates that the change to the linker is a failure. Preliminary results suggested that the phenyl 1,2,3-triazole groups would improve the anti-proliferative activities of oridonin, highlighting the importance of the linker.

As we can see in Table 1, all the compounds **C1-C9**, with different substituted indole-2-carboxylic acids, were slightly more potent against HCT116, MCF-7, and BEL7402 cells than oridonin and 5-Fu. They exhibited better anti-proliferative activities ($IC_{50}$ = 2.64 $\mu$M, 1.64 $\mu$M, 0.81 $\mu$M, 0.29 $\mu$M, 0.82 $\mu$M, 0.68 $\mu$M, 0.16 $\mu$M, 1.67 $\mu$M, and 0.55 $\mu$M, respectively) than oridonin ($IC_{50}$ = 6.84 $\mu$M) in HCT116 cells. The order of activity was *6*-$OCH_3$ > *6*-F > *4,5,6*-$OCH_3$ > *6*-Br > *5*-$OCH_3$ ≈ *6*-Cl > *5*-Cl ≈ *5,6*-$OCH_3$ > *5*-H. Similarly, compounds **C1-C9** displayed lower $IC_{50}$ values (0.39-2.45 $\mu$M) than oridonin (17.56 μM) in MCF-7 cells. Moreover, they were more potent than oridonin ($IC_{50}$ = 9.59 $\mu$M) against BEL7402 cells with $IC_{50}$ values ranging from 0.83 $\mu$M to 3.03 $\mu$M. In order to explore the importance of the indole-2-yl group for the anti-proliferative activity, we designed and synthesised compounds **D1**, **D2**, **E**, and **F** by replacing it with N-methyl-indole-3-yl, indole-3-yl, quinoline ring, and isoquinoline ring, respectively. The pharmacological results of these compounds are shown in Table 1. Compounds **D1**, **E**, and **F** exhibited potent anti-proliferative efficacy against HCT116, MCF-7, BEL7402 cancer cell lines, with $IC_{50}$ values ranging from 1.17 $\mu$M to 2.51 $\mu$M, 0.41 $\mu$M to 0.95 $\mu$M, and 2.30 $\mu$M to 3.95 $\mu$M, respectively. Their anti-proliferative activity was similar to that of compound **C1** with $IC_{50}$ values of 2.64 $\mu$M, 0.78 $\mu$M, and 3.12 $\mu$M, respectively. However, compound **D2** showed lower anti-proliferative activity than C1 with $IC_{50}$ values of 2.73 $\mu$M, 3.81 $\mu$M, and 5.31 $\mu$M, respectively. The results suggested that, compared with indole-2-yl, N-methyl-indole-3-yl, quinoline ring and isoquinoline ring can also greatly improve the anti-proliferative activity of oridonin. Therefore, we believe that compounds **D1**, **E**, and **F** could be potential lead compounds for further optimisation. Based on the preliminary results above, a general SAR was established (Figure 3). Among all target

compounds, compounds **C1**, **C3-C8**, **F**, and **G** exhibited a remarkable anti-proliferative efficacy with $IC_{50}$ < 1.0 $\mu$M; we defined them as potential compounds and conducted more in-depth research on them. Notably, compound **C3**, with a 5-methoxyindole-2-acid substituent, exhibited potent anti-proliferative efficacy against HCT116, MCF-7, and BEL7402 cancer cell lines with $IC_{50}$ values of 0.81 $\mu$M, 0.39 $\mu$M, and 0.83 $\mu$M, respectively, showing efficient and broad-spectrum anti-proliferative activity. Regarding compound **C7** with a 6-methoxyindole-2-acid substituent, it exhibited the strongest activity against HCT116 cells in all compounds; it was about 43- and 155-fold more efficacious than oridonin ($IC_{50}$ = 6.84 $\mu$M) and 5-Fu ($IC_{50}$ = 24.80 $\mu$M).

*2.2.2 Selective inhibition of cancer cell growth by compounds **C1**, **C3-C8**, **E**, and **F** in vitro*

The lack of selectivity between normal and cancer cells is one of the main limitations of antitumour drugs [56]. Therefore, we evaluated the cytotoxicity of compounds **C1**, **C3-C8**, **E**, and **F** in normal cell lines L02 (human normal liver cells) in order to determine the selectivity index (ratio of cytotoxicity in L02 cells compared to that in cancer cells). As shown in Table 2, compound **C7** exhibited a 23.6-fold higher selectivity for HCT116 cells than for normal L02 cells; this selectivity was significantly higher than that exhibited by oridonin and 5-Fu. Compound **C7** not only exhibited the strongest anti-proliferative activity against HCT116 cells, but selectively inhibited tumour cells. Therefore, it was chosen for further biological studies.

*2.2.3 Compound **C7** inhibited HCT-116 Cells colony formation*

Malignant tumour cells have the ability to proliferate indefinitely. The colony formation assay is used to determine the colony formation ability of cells [57]. Therefore, we investigated the anti-proliferative efficacy of compound **C7** by performing a colony formation assay. As shown in Figure 4, the exposure of HCT116 cells to compound **C7** significantly decreased the number and size of colonies in a concentration-dependent manner. These data demonstrated that **C7** could efficiently

inhibit colony formation in HCT116 cells.

*2.2.4 Compound **C7** induced cell cycle arrest with a change in the expression of cyclin A and cyclin B1*

Cell cycle dysregulation, uncontrolled mitotic is an important cause of infinite proliferation of cancer cells [58]. Therefore, blocking the cell cycle and inhibiting mitotic division of cells are considered effective to prevent cell proliferation. In order to explore the mechanism of compound **C7** in the inhibition of cancer cell proliferation, we investigated the effect of **C7** on the cell cycle progression using flow cytometry analysis. As illustrated in Figure 5A and 5B, **C7** increased the percentage of cell population in G2/M phase of the cell cycle in a concentration-dependent manner from 11.90% to 39.42% after 24 h incubation compared to cells incubated in DMSO as a vehicle control. Similarly, **C7** increased the percentage of cell population in the S phase of the cell cycle from 23.30% to 29.92%. These results suggested that **C7** could induce cancer cell cycle arrest at the S and G2/M phases.

It has been reported that cyclin A forms a complex with (Cyclin-dependent kinase 1) CDK1 and (Cyclin-dependent kinase 2) CDK2 as a key regulator in the S phase [59]. Cyclin B1, also called maturation or mitosis promoting factor, forms a complex with CDK1. The reduced expression of cyclin B1 complex inhibits cell cycle progression from the G2 phase to the M phase [60]. In order to determine the mechanism of cell cycle arrest by **C7**, we performed western blotting. As shown in Figure 5C and D, treatment with compound **C7** or oridonin for 24 h inhibited the expression of cyclin A and cyclin B1 in a dose-dependent manner compared with the control group. At the same concentration (3 $\mu$M), the effect of compound **C7** on the expression of proteins was significantly stronger than that of oridonin ($p < 0.001$).

*2.2.5 Compound **C7**-induced morphological changes in HCT116 cells by haematoxylin and eosin (H&E) staining*

The mechanism of action of many anti-proliferative drugs is to induce apoptosis. Cells that undergo apoptosis generally undergo morphological changes [61].

Therefore, we used H&E staining to assess the morphological changes in cells. As shown in Figure 6, HCT116 cells incubated with **C7** or oridonin for 24 h displayed significant apoptotic morphological changes such as loss of the original morphology, unstructured state, volume swelling, cell condensed nuclei, cell lysis, and membrane shrinkage. These results suggest that **C7** has stronger effects on cell morphology than oridonin at the same concentration (1 $\mu$M).

*2.2.6 Compound **C7**-induced cancer cell apoptosis with a change in the expression of apoptosis-related proteins*

To further confirm that **C7** could induce apoptosis, vehicle-, **C7**-, or oridonin-incubated HCT116 cells were stained with Annexin V and PI. As shown in Figure 7A and B, incubation with **C7** (0.03, 0.10, 0.30, 1.00, 3.00 $\mu$M) induced a concentration-dependent increase in the percentage of total apoptotic (early and late stage) cells from 14.02% to 94.8% (3.00 $\mu$M). This result indicates that compound **C7** induces apoptosis.

Bcl-2 family proteins including pro-apoptotic (e.g., Bax) and anti-apoptotic proteins (e.g., Bcl-2) are key regulators of apoptosis. The upregulation or downregulation of apoptotic genes will promote or inhibit cell apoptosis [62]. The caspase family exhibits important functions in the regulation process of cell apoptosis. For example, caspase-9 is one of the initiators of apoptosis and caspase-3 is one of the activators of apoptosis [62]. As shown in Figure 8C, the expression of Bax increased after treatment with compound **C7** for 24 h at concentrations $\geq$ 0.10 $\mu$M, while Bcl-2 expression significantly decreased in a concentration-dependent manner (Figure 7D). Furthermore, pro-apoptotic proteins caspase-9 and caspase-3 increased in a concentration-dependent manner after treatment with **C7** for 24 h (Figure 7C and D). These results indicate that **C7** significantly inhibits the growth of HCT116 cells by inducing apoptosis through the caspase-dependent pathway and increasing the Bax/Bcl2 ratio. The effect of **C7** on the expression level of Bcl-2, Bax, caspase-9 and caspase-3 in HCT116 cells was more pronounced at the same concentration of 3.00 $\mu$M ($p < 0.001$, Figure 7D) than that of oridonin. This also explains that compound **C7** has better antitumour activity than oridonin.

*2.2.7 Effect of compound **C7** on the expression of p53-related proteins*

To date, there have been many reports on the mechanism of action of Rubescensine A. The molecular mechanism of its antitumour activity involves reactive oxygen species (ROS), Bcl-2/Bax, NF-κB, p53/p21, MAPK, PI3K, microRNA, and fatty acid synthase pathways [63,64]. Among them, the p53/p21 signalling pathway attracted our interest because it plays a key role in both cell cycle arrest and apoptosis. P53, known as the "guardian of genome", is a powerful tumour suppressor encoded by the p53 gene. It promotes the expression of functional p53 and results in antitumour effects [65]. It has previously been reported that p53 transactivates p21, directly binding and inhibiting the expression of cyclin B1/CDK1 complex, thus inducing G2/M phase arrest. It can also initiate apoptosis by upregulating Bax while downregulating Bcl-2 expression, which contributes to the activation of caspase-9 and caspase-3 [66]. In addition, ubiquitin ligase murine double minute chromosome 2 (MDM2) is a key negative regulator of p53 expression [65]. Recently, it has become an important target for antitumour drugs and many MDM2 inhibitor molecules have entered clinical research [67-70].

Preliminary results indicate that compound **C7** can induce cell cycle arrest by affecting cyclin family proteins and apoptosis through Bcl-2/Bax/Caspase signalling. Therefore, we suspect that **C7** may inhibit cell proliferation by regulating the p53/p21 signalling pathway. In order to explore its mechanism of action, western blotting was performed to determine the expression of p21, p53, and MDM2. As shown in Figure 8A and B, compound **C7** inhibited the expression of MDM2 at concentrations greater than 0.10 $\mu$M, upregulating the expression of p53 and p21 compared to that in the control group. Moreover, it acts better on these proteins than oridonin at 3.00 $\mu$M. It suggested that the p53-MDM2 pathway may be involved in **C7** induced the arrest of G2/M phase and apoptosis in HCT116 cancer cells.

*2.2.8. In vivo antitumour activity of compound **C7***

To evaluate the antitumour activity of compound **C7** *in vivo*, a colon cancer xenograft

model was established by subcutaneous inoculation of HCT116 cells into nude mice. The mice were sorted into four experimental groups (six animals per group) and one control group, oridonin-, **C7**-, and paclitaxel-treated mice received a vehicle solution, 25 mg/kg of oridonin, 25 mg/kg of compound **C7**, and 25 mg/kg of paclitaxel. The tumour size and body weight of the mice were recorded every two days. At the end of the treatment, the mice were sacrificed and the tumours were recovered and separately weighed. As shown in Figure 9, average volume and weight of the tumour in oridonin-, **C7**-, and paclitaxel-treated groups were significantly lower than those in the control group. The tumour growth inhibition rates in mice treated with oridonin, **C7,** and paclitaxel were 58.61%, 85.82%, and 90.57%, respectively. However, in this group, the body weight of mice changed slightly compared to that in the control group with no statistically significant difference. Based on the above pharmacological data, the antitumour activity of compound **C7** was significantly stronger than that of oridonin and lower than that of the positive control paclitaxel *in vivo*.

## 3. Conclusions

In this study, 25 novel C-14 derivatives of oridonin were designed, synthesised, and biologically evaluated. Most of them displayed significantly enhanced anti-proliferative efficacy in a panel of human cancer cell lines. SAR analysis indicated that the target compounds containing an indole ring exhibited more remarkable anti-proliferative activity than the target compounds containing phenyl 1, 2, 3-triazole. Among these molecules, compound **C7** with a 6-methoxyindole-2-acid substituent, displayed the most potent inhibitory activity against HCT116 cell lines with an $IC_{50}$ value of 0.16 $\mu$M (43-fold more potent than oridonin). Particularly, the $IC_{50}$ value of **C7** in L02 normal cells was 23.6-fold higher than that in HCT116 cells, indicating its selective anti-proliferative effects. In addition, compound **C7** can inhibit the colony formation of HCT116 cells in a concentration-dependent manner.

Furthermore, cell cycle arrest and apoptosis induced by compound **C7** may be achieved through the p53-MDM2 signalling pathway; this involves inhibition of the

expression of cyclin A and cyclin B1 and regulation of the expression of Bcl and caspase family proteins. Moreover, compound **C7** significantly suppressed the tumour volume and reduced its weight by 85.82% at a dose of 25 mg/kg/day (iv) in an HCT116 colon cancer xenograft model, compared to oridonin (58.61%).

In summary, compound **C7** showed an outstanding antitumour activity both *in vivo* and *in vitro* and has the potential to be further developed into a promising antitumor compound.

## 4. Experimental section

All chemicals were purchased from commercial source and used without further purification unless otherwise stated. The reactions were monitored by TLC using Merck Kieselgel 60 F 254 plates and visualized under UV light at 254 nm. Column chromatography was generally performed on silica gel (200 mesh size).[1] H-NMR and $^{13}$ C-NMR spectra were measured on an AV-300 (Bruker BioSpin, Switzerland) and AV-500 (Bruker BioSpin, Switzerland), and all chemical shifts were given in ppm relative to tetramethylsilane (TMS). High-resolution mass spectra (HRMS) were measured with an Thermo Scientific LTQ Orbitrap XL in ESI mode.

### *4.1 General procedure for the reaction of oridonin with different intermediates containing-carboxyl*

To a solution of oridonin (36.4 mg, 0.1 mmol) in 10 mL dry $CH_2Cl_2$ and different carboxyl compounds (0.15 mmol), the solution was treated with EDCI (0.3 mmol) and 4-dimethylaminopyridine (DMAP) (10 mg). The mixture was stirred at 25 ℃ for 2-8 h and monitored by TLC. After completion of the reaction, water was added and the mixture was extracted with dichloromethane and the organic phase was washed with saturated sodium bicarbonate solution and brine, and dried over $Na_2SO_4$. The evaporation of the solvents gave the crude products, which were purified by silica gel column ($CH_2Cl_2$/MeOH, 100:1) to afford compounds **A1-9**, **B1-3**, **C1-9**, **D1**, **E**, **F.**

#### *4.1.1 (1S,4aR,5S,6S,6aR,9S,11aS,14R)-1,5,6-trihydroxy-4,4-dimethyl-8-methylene-7-*

*oxododecahydro-1H-6,11b-(epoxymethano)-6a,9-methanocyclohepta[a]naphthalen-14-yl 1-phenyl-1H-1,2,3-triazole-4-carboxylate* ***(A1)***

White powder; yield 69%. $[a]_D^{25}$ -57 (c 0.09, $CH_3OH$); $^1H$ NMR (300 MHz, DMSO-$d_6$, ppm) $\delta$ 9.14 (s, 1H), 7.93 (d, *J* = 7.7 Hz, 2H), 7.66-7.51 (m, 3H), 6.09 (d, *J* = 10.1 Hz, 2H), 5.93 (d, *J* = 10.3 Hz, 1H), 5.88 (s, 1H), 5.68 (s, 1H), 4.46 (t, *J* = 7.4 Hz, 1H), 4.16 (d, *J* = 10.1 Hz, 1H), 3.87 (d, *J* = 10.0 Hz, 1H), 3.50 (dd, *J* = 9.8, 6.9 Hz, 1H), 3.22 (d, *J* = 9.8 Hz, 1H), 2.59 (dd, *J* = 14.4, 6.8 Hz, 1H), 2.19 (ddd, *J* = 22.8, 15.3, 8.2 Hz, 1H), 1.94 (dd, *J* = 12.9, 5.8 Hz, 1H), 1.79-1.67 (m, 1H), 1.50 (dd, *J* = 26.4, 13.9 Hz, 3H), 1.34-1.14 (m, 4H), 1.00 (s, 6H). $^{13}C$ NMR (75 MHz, DMSO-$d_6$) $\delta$ 207.12, 158.88, 150.35, 140.03, 135.98, 129.87 (2C), 129.37, 127.21, 120.76 (2C), 119.84, 95.78, 74.96, 74.01, 71.50, 62.68, 62.06, 59.15, 53.99, 41.19, 40.50, 38.30, 33.32, 32.65, 30.42, 29.32, 21.57, 19.63. ESI-HRMS calcd for $C_{29}H_{34}N_3O_7^+$ ($[M+H]^+$): 536.2391; found: 536.2390.

*4.1.2 (1S,4aR,5S,6S,6aR,9S,11aS,14R)-1,5,6-trihydroxy-4,4-dimethyl-8-methylene-7-oxododecahydro-1H-6,11b-(epoxymethano)-6a,9-methanocyclohepta[a]naphthalen-14-yl 1-(2-fluorophenyl)-1H-1,2,3-triazole-4-carboxylate* ***(A2)***

White powder; yield 82%; $[a]_D^{25}$ -85 (c 0.11, $CH_3OH$); $^1H$ NMR (300 MHz, DMSO-$d_6$, ppm) $\delta$ 8.91 (s, 1H), 7.83 (t, *J* = 7.7 Hz, 1H), 7.71-7.53 (m, 2H), 7.47 (d, *J* = 7.5 Hz, 1H), 6.11 (s, 1H), 6.05 (s, 1H), 5.93-5.83 (m, 2H), 5.67 (s, 1H), 4.42 (d, *J* = 5.0 Hz, 1H), 4.16 (d, *J* = 10.1 Hz, 1H), 3.87 (d, *J* = 9.9 Hz, 1H), 3.51 (dd, *J* = 10.2, 6.9 Hz, 1H), 3.43-3.34 (m, 1H), 3.21 (d, *J* = 9.4 Hz, 1H), 2.26-2.10 (m, 1H), 1.97-1.91 (d, 1H), 1.82-1.70 (m, 1H), 1.57-1.4 (m, 3H), 1.36-1.10 (m, 4H), 1.00 (d, *J* = 2.2 Hz, 6H). $^{13}C$ NMR (75 MHz, DMSO-*d6*, ppm) $\delta$ 207.54, 154.59 (d, *J* = 249.6 Hz, 1C), 150.90, 140.12, 132.51 (d, *J* = 8.49 Hz, 1H), 130.97, 126.92, 126.0170, 125.97, 124.55 (d, *J* = 10.88 Hz, 1C) 120.22, 117.54 (d, *J* = 19.16 Hz, 1C), 96.27, 75.33, 74.46, 72.02, 63.13, 62.54, 59.63, 54.45, 41.71, 40.99, 38.79, 33.78, 33.12, 30.86, 29.78, 22.05, 20.12. ESI-HRMS calcd for $C_{29}H_{32}FN_3O_7^+$ ($[M+H]^+$): 554.2297; found: 554.2294.

*4.1.3 (1S,4aR,5S,6S,6aR,9S,11aS,14R)-1,5,6-trihydroxy-4,4-dimethyl-8-methylene-7-oxododecahydro-1H-6,11b-(epoxymethano)-6a,9-methanocyclohepta[a]naphthalen-14-yl 1-(4-fluorophenyl)-1H-1,2,3-triazole-4-carboxylate* ***(A3)***

White powder; yield 70%; $[a]_D^{25}$ -78 (c 0.12, $CH_3OH$); $^1H$ NMR (300 MHz, DMSO-$d_6$, ppm) $\delta$ 9.12 (s, 1H), 7.99 (dd, $J$ = 9.0, 4.7 Hz, 2H), 7.49 (d, $J$ = 8.8 Hz, 2H), 6.09 (d, $J$ = 11.5 Hz, 2H), 5.91 (d, $J$ = 10.2 Hz, 1H), 5.86 (s, 1H), 5.68 (s, 1H), 4.45 (d, $J$ = 5.0 Hz, 1H), 4.16 (d, $J$ = 10.7 Hz, 1H), 3.87 (d, $J$ = 9.8 Hz, 1H), 3.50 (s, 1H), 3.42-3.38 (m, 1H), 3.21 (d, $J$ = 9.7 Hz, 1H), 2.23-2.15 (s, 1H), 1.98-1.92 (m, 1H), 1.78-1.73 (m, 1H), 1.55-1.47 (m, 3H), $^{13}C$ NMR (126 MHz, DMSO-$d_6$, ppm) $\delta$ 207.91, 159.40, 150.47, 140.38, 132.81, 127.91, 123.84 (2C), 123.77, 120.80, 117.36 (2C), 117.17, 96.19, 75.77, 74.45, 72.08, 63.18, 62.51, 59.63, 54.41, 41.57, 40.97, 38.61, 33.67, 32.94, 30.71, 29.56, 21.82, 19.95. 1.31-1.17 (m, 4H), 1.00 (s, 6H). ESI-HRMS calcd for $C_{29}H_{32}FN_3O_7^+$ ($[M+H]^+$): 554.2297; found: 554.2296.

*4.1.4 (1S,4aR,5S,6S,6aR,9S,11aS,14R)-1,5,6-trihydroxy-4,4-dimethyl-8-methylene-7-oxododecahydro-1H-6,11b-(epoxymethano)-6a,9-methanocyclohepta[a]naphthalen-14-yl 1-(4-chlorophenyl)-1H-1,2,3-triazole-4-carboxylate* ***(A4)***

White powder; Yield 78%; $[a]_D^{25}$ -88 (c 0.08, $CH_3OH$); $^1H$ NMR (300 MHz, DMSO-$d_6$, ppm) $\delta$ 9.17 (s, 1H), 7.99 (d, $J$ = 8.8 Hz, 2H), 7.69 (d, $J$ = 8.8 Hz, 2H), 6.09 (d, $J$ = 12.6 Hz, 2H), 5.91 (d, $J$ = 10.3 Hz, 1H), 5.86 (s, 1H), 5.68 (s, 1H), 4.44 (d, $J$ = 4.9 Hz, 1H), 4.15 (d, $J$ = 10.9 Hz, 1H), 3.87 (d, $J$ = 10.6 Hz, 1H), 3.50 (dd, $J$ = 10.2, 7.0 Hz, 2H), 3.21 (d, $J$ = 9.4 Hz, 1H), 2.19 (s, 1H), 1.98-1.91 (m, 1H), 1.78-1.72 (m, 1H), 1.53-1.45 (s, 3H), 1.30-1.16 (m, 4H), 1.00 (s, 6H). $^{13}C$ NMR (126 MHz, DMSO-$d_6$, ppm) $\delta$ 207.59, 159.30, 150.83, 140.62, 135.29, 134.22, 130.32 (2C), 127.81, 123.05 (2C), 120.36, 96.26, 75.45, 74.50, 72.00, 63.15, 62.55, 59.63, 54.49, 41.68, 41.00, 38.78, 33.79, 33.13, 30.91, 29.78, 22.05, 20.11. ESI-HRMS calcd for $C_{29}H_{33}ClN_3O_7^+$ ($[M+H]^+$): 570.2002; found: 570.1999.

*4.1.5 (1S,4aR,5S,6S,6aR,9S,11aS,14R)-1,5,6-trihydroxy-4,4-dimethyl-8-methylene-7-oxododecahydro-1H-6,11b-(epoxymethano)-6a,9-methanocyclohepta[a]naphthalen-*

*14-yl 1-(p-tolyl)-1H-1,2,3-triazole-4-carboxylate* ***(A5)***

White powder; Yield 81%; $[a]_D^{25}$ -92 (c 0.11, $CH_3OH$); $^1H$ NMR (300 MHz, DMSO-$d_6$, ppm) $\delta$ 9.08 (s, 1H), 7.81 (d, $J$ = 8.5 Hz, 2H), 7.41 (d, $J$ = 8.5 Hz, 2H), 6.08 (d, $J$ = 8.7 Hz, 2H), 5.92 (d, $J$ = 10.3 Hz, 1H), 5.87 (s, 1H), 5.68 (s, 1H), 4.44 (d, $J$ = 5.0 Hz, 1H), 4.16 (d, $J$ = 10.1 Hz, 1H), 3.89 (s, 1H), 3.56-3.46 (m, 1H), 3.42-3.38 (m, 1H), 3.22 (d, $J$ = 9.8 Hz, 1H), 2.39 (s, 3H), 2.28-2.14 (m, 1H), 2.05-1.89 (m, 1H), 1.74 (dd, $J$ = 16.9, 8.9 Hz, 1H), 1.60-1.45 (m, 3H), 1.23-1.12 (m, 4H), 1.00 (s, 6H). $^{13}C$ NMR (126 MHz, DMSO-$d_6$, ppm) $\delta$ 207.63, 159.40, 150.86, 140.42, 139.60, 134.23, 130.70 (2C), 127.49, 121.10 (2C), 120.30, 96.27, 75.45, 74.50, 71.99, 63.16, 62.55, 59.66, 54.47, 41.68, 41.01, 38.80, 33.80, 33.13, 30.91, 29.80, 22.06, 21.08, 20.10. ESI-HRMS calcd for $C_{30}H_{36}N_3O_7^+$ ($[M+H]^+$): 550.2548; found: 550.2546.

*4.1.6 (1S,4aR,5S,6S,6aR,9S,11aS,14R)-1,5,6-trihydroxy-4,4-dimethyl-8-methylene-7-oxododecahydro-1H-6,11b-(epoxymethano)-6a,9-methanocyclohepta[a]naphthalen-14-yl 1-(4-methoxyphenyl)-1H-1,2,3-triazole-4-carboxylate* ***(A6)***

White powder; yield 84%; $[a]_D^{25}$ -77 (c 0.07, $CH_3OH$); $^1H$ NMR (300 MHz, DMSO-$d_6$, ppm) $\delta$ 9.03 (s, 1H), 7.83 (d, $J$ = 9.0 Hz, 2H), 7.14 (d, $J$ = 9.1 Hz, 2H), 6.08 (d, $J$ = 7.8 Hz, 2H), 5.92 (d, $J$ = 10.1 Hz, 1H), 5.86 (s, 1H), 5.68 (s, 1H), 4.45 (d, $J$ = 4.6 Hz, 1H), 4.15 (d, $J$ = 10.2 Hz, 1H), 3.86 (s, 1H), 3.84 (s, 3H), 3.49 (dd, $J$ = 9.5, 6.0 Hz, 1H), 3.22 (d, $J$ = 9.6 Hz, 1H), 2.61 (dd, $J$ = 11.8, 5.6 Hz, 1H), 2.24-2.14 (m, 1H), 1.99-1.92 (m, 1H), 1.78-1.70 (m, 1H), 1.57-1.46 (m, 3H), 1.32-1.17 (m, 4H), 1.00 (s, 6H). $^{13}C$ NMR (75 MHz, DMSO-$d_6$, ppm) $\delta$ 207.64, 160.25, 159.43, 150.84, 140.28, 129.79, 127.57, 122.96 (2C), 120.30, 115.33 (2C), 96.27, 75.48, 74.47, 71.99, 63.16, 62.53, 59.66, 56.09, 54.46, 41.66, 40.99, 38.78, 33.79, 33.11, 30.89, 29.78, 22.03, 20.07. ESI-HRMS calcd for $C_{30}H_{36}N_3O_8^+$ ($[M+H]^+$): 566.2497; found: 566.2492.

*4.1.7 (1S,4aR,5S,6S,6aR,9S,11aS)-1,5,6-trihydroxy-4,4-dimethyl-8-methylene-7-oxododecahydro-1H-6,11b-(epoxymethano)-6a,9-methanocyclohepta[a]naphthalen-14-yl 1-(3,4-dimethoxyphenyl)-1H-1,2,3-triazole-4-carboxylate* ***(A7)***

White powder; yield 75%; $[a]_D^{25}$ -66 (c 0.05, $CH_3OH$); $^1H$ NMR (300 MHz, DMSO-$d_6$, ppm) $\delta$ 9.09 (s, 1H), 7.46 (dd, *J* = 10.7, 5.7 Hz, 2H), 7.13 (d, *J* = 8.7 Hz, 1H), 6.09 (d, *J* = 11.4 Hz, 2H), 5.92 (d, *J* = 10.2 Hz, 1H), 5.83 (s, 1H), 5.69 (s, 1H), 4.45 (d, *J* = 4.9 Hz, 1H), 4.16 (d, *J* = 10.0 Hz, 1H), 3.89 (s, 1H), 3.86 (s, 3H), 3.82 (d, *J* = 4.0 Hz, 3H), 3.55-3.47 (m, 1H), 3.22 (d, *J* = 9.6 Hz, 1H), 2.54 (s, 1H), 2.21 (dd, *J* = 16.3, 8.9 Hz, 1H), 1.96 (dd, *J* = 13.0, 6.1 Hz, 1H), 1.73 (dd, *J* = 14.7, 8.2 Hz, 1H), 1.58-1.44 (m, 3H), 1.34-1.17 (m, 4H), 1.00 (s, 6H). $^{13}C$ NMR (75 MHz, DMSO-$d_6$, ppm) $\delta$ 207.64, 159.47, 150.83, 149.89, 149.75, 140.22, 129.78, 127.65, 120.34, 113.58, 112.39, 105.82, 96.29, 75.53, 74.43, 71.99, 63.17, 62.52, 59.69, 56.46, 56.32, 54.48, 41.65, 41.00, 38.77, 33.80, 33.11, 30.93, 29.79, 22.03, 20.07. ESI-HRMS calcd for $C_{31}H_{38}N_3O_9^+$ ($[M+H]^+$): 596.2603; found: 596.2600.

*4.1.8 (1S,4aR,5S,6S,6aR,9S,11aS,14R)-1,5,6-trihydroxy-4,4-dimethyl-8-methylene-7-oxododecahydro-1H-6,11b-(epoxymethano)-6a,9-methanocyclohepta[a]naphthalen-14-yl 1-(3,4,5-trimethoxyphenyl)-1H-1,2,3-triazole-4-carboxylate* ***(A8)***

White powder; yield 77%; $[a]_D^{25}$ -175 (c 0.02, $CH_3OH$); $^1H$ NMR (300 MHz, DMSO-$d_6$, ppm) $\delta$ 9.18 (s, 1H), 7.22 (s, 2H), 6.10 (d, *J* = 15.9 Hz, 2H), 5.91 (d, *J* = 10.3 Hz, 1H), 5.82 (s, 1H), 5.69 (s, 1H), 4.45 (d, *J* = 4.7 Hz, 1H), 4.16 (d, *J* = 9.8 Hz, 1H), 3.87 (s, 7H), 3.77 (d, *J* = 6.0 Hz, 1H), 3.71 (s, 3H), 3.51 (s, 1H), 3.23 (d, *J* = 8.9 Hz, 1H), 2.65 (d, *J* = 14.1 Hz, 1H), 2.24 – 2.12 (m, 1H), 1.97 (s, 2H), 1.79-1.71 (m, 1H), 1.58-1.42 (m, 3H), 1.34-1.17 (m, 4H), 1.00 (s, 6H). $^{13}C$ NMR (75 MHz, DMSO-$d_6$, ppm) $\delta$ 207.64, 159.47, 153.95, 150.81, 140.29, 138.44, 132.30, 127.90, 120.37, 99.51, 96.31, 75.58, 74.41, 71.98, 63.17, 62.51, 60.67, 59.70, 56.88, 54.51, 41.66, 41.01, 38.79, 33.80, 33.10, 31.14, 29.79, 24.21, 22.03. ESI-HRMS calcd for $C_{32}H_{40}N_3O_{10}^+$ ($[M+H]^+$): 626.2708; found: 626.2707.

*4.1.9 (1S,4aR,5S,6S,6aR,9S,11aS,14R)-1,5,6-trihydroxy-4,4-dimethyl-8-methylene-7-oxododecahydro-1H-6,11b-(epoxymethano)-6a,9-methanocyclohepta[a]naphthalen-14-yl 1-(4-nitrophenyl)-1H-1,2,3-triazole-4-carboxylate* ***(A9)***

White powder; yield 64%; $[a]_D^{25}$ -47 (c 0.08, $CH_3OH$); $^1H$ NMR (300 MHz, DMSO-$d_6$, ppm) $\delta$ 9.35 (s, 1H), 8.46 (d, $J$ = 9.1 Hz, 2H), 8.28 (d, $J$ = 9.1 Hz, 2H), 6.11 (d, $J$ = 16.9 Hz, 2H), 5.91 (d, $J$ = 10.4 Hz, 1H), 5.87 (s, 1H), 5.69 (s, 1H), 4.45 (d, $J$ = 4.9 Hz, 1H), 4.16 (d, $J$ = 10.1 Hz, 1H), 3.92-3.85 (m, 1H), 3.52 (d, $J$ = 6.9 Hz, 1H), 3.22 (d, $J$ = 8.8 Hz, 1H), 2.60 (s, 1H), 2.25-2.12 (m, 1H), 2.02-1.90 (m, 1H), 1.79-1.71 (m, 1H), 1.58-1.44 (m, 3H), 1.37-1.14 (m, 4H), 1.01 (s, 6H). $^{13}C$ NMR (126 MHz, DMSO-$d_6$, ppm) $\delta$ 207.52, 159.17, 150.86, 147.70, 140.99, 140.76, 128.18, 125.90 (2C), 122.03 (2C), 120.37, 96.28, 75.45, 74.53, 72.01, 63.13, 62.58, 59.61, 54.54, 41.71, 41.01, 38.80, 33.80, 33.16, 30.96, 29.80, 22.08, 20.13. ESI-HRMS calcd for $C_{29}H_{33}N_4O_9^+$ ($[M+H]^+$): 581.2242; found: 581.2240.

*4.1.10 (1S,4aR,5S,6S,6aR,9S,11aS,14R)-1,5,6-trihydroxy-4,4-dimethyl-8-methylene-7-oxododecahydro-1H-6,11b-(epoxymethano)-6a,9-methanocyclohepta[a]naphthalen-14-yl 4-oxo-4-(((1-phenyl-1H-1,2,3-triazol-4-yl)methyl)amino)butanoate* ***(B1)***

White powder; yield 43%; $[a]_D^{25}$ -57 (c 0.10, $CH_3OH$); $^1H$-NMR (300 MHz, DMSO-$d_6$, ppm): $\delta$ 8.59 (s, 1H), 8.43 (s, 1H), 7.89 (d, $J$ = 7.5 Hz, 2H), 7.60 (t, $J$ = 7.7 Hz, 2H), 7.49 (d, $J$ = 7.4 Hz, 1H), 6.00 (s, 1H), 5.89 (t, $J$ = 10.3 Hz, 2H), 5.60 (s, 1H), 4.42 (d, J = 4.9 Hz, 1H), 4.37 (d, $J$ = 5.0 Hz, 2H), 4.07 (d, $J$ = 10.3 Hz, 1H), 3.82 (d, $J$ = 9.9 Hz, 1H), 3.59-3.46 (m, 2H), 2.95 (d, $J$ = 9.9 Hz, 1H), 2.46-2.24 (m, 4H), 2.05 (s, 1H), 1.91-1.79 (m, 1H), 1.69 (d, J = 13.9 Hz, 1H), 1.44 (dd, $J$ = 21.3, 13.3 Hz, 4H), 1.35-1.17 (m, 4H), 0.99 (s, 6H). $^{13}C$-NMR (75 MHz, DMSO-$d_6$, ppm): $\delta$ 207.64, 171.61, 171.38, 151.19, 146.72, 137.13, 130.36 (2C), 129.03, 121.47, 120.35 (2C), 96.16, 74.54, 73.88, 72.01, 62.99, 62.27, 59.53, 54.30, 41.73, 40.92, 38.80, 34.70, 33.78 (2C), 33.16, 30.73, 30.17 (2C), 29.79, 22.10, 20.15. ESI-HRMS calcd for $C_{33}H_{41}N_4O_8^+$ ($[M+H]^+$): 621.2919; found: 621.2922.

*4.1.11 (1S,4aR,5S,6S,6aR,9S,11aS,14R)-1,5,6-trihydroxy-4,4-dimethyl-8-methylene-7-oxododecahydro-1H-6,11b-(epoxymethano)-6a,9-methanocyclohepta[a]naphthalen-14-yl 4-(((1-(4-chlorophenyl)-1H-1,2,3-triazol-4-yl)methyl)amino)-4-oxobutanoate* ***(B2)***

White powder; yield 40%; $[a]_D^{25}$ -68 (c 0.09, $CH_3OH$); $^1H$ NMR (300 MHz, DMSO-$d_6$, ppm) $\delta$ 8.62 (s, 1H), 8.42 (s, 1H), 7.93 (d, $J$ = 8.9 Hz, 2H), 7.66 (d, $J$ = 8.9 Hz, 2H), 5.99 (s, 1H), 5.88 (dd, $J$ = 11.5, 9.3 Hz, 2H), 5.59 (s, 1H), 4.41 (d, $J$ = 5.0 Hz, 1H), 4.36 (d, $J$ = 5.3 Hz, 2H), 4.10 (d, $J$ = 5.3 Hz, 1H), 3.82 (d, $J$ = 10.1 Hz, 1H), 3.52 (dd, $J$ = 18.2, 11.1 Hz, 2H), 2.95 (d, $J$ = 9.7 Hz, 1H), 2.38 (s, 4H), 2.11-1.97 (m, 1H), 1.85 (s, 1H), 1.70 (dd, $J$ = 18.8, 7.1 Hz, 1H), 1.61-1.35 (m, 4H), 1.35-1.12 (m, 4H), 0.99 (s, 6H). $^{13}C$ NMR (126 MHz, DMSO-$d_6$, ppm) $\delta$ 207.87, 171.96, 171.79, 150.89, 146.78, 135.75, 133.51, 130.36 (2C), 122.16 (2C), 121.64, 120.32, 96.08, 74.54, 74.13, 72.07, 63.02, 62.25, 59.55, 54.29, 43.17, 41.63, 40.89, 38.67, 34.63, 33.68, 33.02, 30.58, 30.13, 29.62, 21.92, 20.03. ESI-HRMS calcd for $C_{33}H_{40}ClN_4O_8^+$ ($[M+H]^+$): 655.2529; found: 655.2527.

*4.1.12 (1S,4aR,5S,6S,6aR,9S,11aS,14R)-1,5,6-trihydroxy-4,4-dimethyl-8-methylene-7-oxododecahydro-1H-6,11b-(epoxymethano)-6a,9-methanocyclohepta[a]naphthalen-14-yl 4-(((1-(4-methoxyphenyl)-1H-1,2,3-triazol-4-yl)methyl)amino)-4-oxobutanoate* ***(B3)***

White powder; yield 52%; $[a]_D^{25}$ -43 (c 0.07, $CH_3OH$); $^1H$ NMR (300 MHz, DMSO-$d_6$, ppm) $\delta$ 8.47 (s, 1H), 8.40 (t, $J$ = 5.5 Hz, 1H), 7.79 (d, $J$ = 8.9 Hz, 2H), 7.13 (d, $J$ = 9.0 Hz, 2H), 6.00 (s, 1H), 5.86 (d, $J$ = 7.8 Hz, 2H), 5.60 (s, 1H), 4.41 (d, $J$ = 5.0 Hz, 1H), 4.35 (d, $J$ = 5.3 Hz, 2H), 4.07 (d, $J$ = 10.2 Hz, 1H), 3.82 (s, 4H), 3.48-3.58 (m, 2H), 2.95 (d, $J$ = 10.4 Hz, 1H), 2.37 (dd, $J$ = 12.3, 6.5 Hz, 4H), 2.04 (d, $J$ = 7.9 Hz, 1H), 1.83 (d, $J$ = 12.6 Hz, 1H), 1.71 (d, $J$ = 7.9 Hz, 1H), 1.56-1.35 (m, 4H), 1.19-1.33 (m, 4H), 0.99 (s, 6H). $^{13}C$ NMR (75 MHz, DMSO-$d_6$, ppm) $\delta$ 207.80, 171.80, 171.78, 159.69, 152.18, 150.96, 146.41, 130.46, 122.13 (2C), 121.52, 115.36 (2C), 97.35, 96.10, 74.54, 74.05, 72.05, 63.01, 62.25, 61.99, 59.54, 55.99, 54.30, 43.11, 41.66, 40.90, 34.70, 33.71, 33.06, 30.63, 30.14, 29.66, 22.05, 21.98, 20.07. ESI-HRMS calcd for $C_{34}H_{43}N4O_9^+$ ($[M+H]^+$): 651.3025; found: 651.3024.

*4.2.13 (1S,4aR,5S,6S,6aR,9S,11aS,14R)-1,5,6-trihydroxy-4,4-dimethyl-8-methylene-7-oxododecahydro-1H-6,11b-(epoxymethano)-6a,9-methanocyclohepta[a]naphthalen-14-yl 1H-indole-2-carboxylate* ***(C1)***

White powder; yield 81%; $[a]_D^{25}$ -70 (c 0.09, $CH_3OH$); $^1H$ NMR (300 MHz, DMSO-$d_6$, ppm) $\delta$ 11.63 (s, 1H), 7.63 (d, $J$ = 7.9 Hz, 1H), 7.45 (d, $J$ = 8.2 Hz, 1H), 7.33-7.19 (m, 1H), 7.05 (t, $J$ = 7.5 Hz, 1H), 6.95 (s, 1H), 6.07 (d, $J$ = 5.6 Hz, 2H), 5.94 (d, $J$ = 10.4 Hz, 1H), 5.91 (s, 1H), 5.67 (s, 1H), 4.45 (d, $J$ = 4.9 Hz, 1H), 4.15 (d, $J$ = 10.0 Hz, 1H), 3.87 (d, $J$ = 10.0 Hz, 1H), 3.52 (dd, $J$ = 10.1, 6.9 Hz, 1H), 3.39 (d, $J$ = 5.0 Hz, 1H), 3.17 (d, $J$ = 6.8 Hz, 1H), 2.15 (dd, $J$ = 21.7, 13.2 Hz, 1H), 1.94 (dd, $J$ = 12.4, 4.8 Hz, 1H), 1.84-1.71 (m, 1H), 1.57-1.44 (m, 3H), 1.41-1.13 (m, 4H), 1.01 (s, 6H). $^{13}C$ NMR (126 MHz, DMSO-$d_6$, ppm) $\delta$ 207.69, 160.67, 151.22, 137.73, 128.20, 127.09, 124.94, 122.49, 120.53, 120.01, 112.98, 108.58, 96.34, 74.68, 74.57, 72.04, 63.08, 62.51, 59.64, 54.48, 41.95, 41.01, 38.83, 33.82, 33.19, 30.83, 29.82, 22.11, 20.21. ESI-HRMS calcd for $C_{29}H_{34}NO_7^+$ ($[M+H]^+$): 508.2330; found: 508.2328.

*4.2.14 (1S,4aR,5S,6S,6aR,9S,11aS,14R)-1,5,6-trihydroxy-4,4-dimethyl-8-methylene-7-oxododecahydro-1H-6,11b-(epoxymethano)-6a,9-methanocyclohepta[a]naphthalen-14-yl 5-chloro-1H-indole-2-carboxylate* ***(C2)***

White powder; yield 83%; $[a]_D^{25}$ -40 (c 0.11, $CH_3OH$); $^1H$ NMR (300 MHz, DMSO-$d_6$, ppm) $\delta$ 11.85 (s, 1H), 7.73 (s, 1H), 7.46 (d, $J$ = 8.7 Hz, 1H), 7.24 (d, $J$ = 8.8 Hz, 1H), 6.92 (s, 1H), 6.08 (s, 2H), 5.93 (t, $J$ = 5.0 Hz, 2H), 5.67 (s, 1H), 4.44 (d, $J$ = 4.9 Hz, 1H), 4.15 (d, $J$ = 10.1 Hz, 1H), 3.87 (d, $J$ = 10.0 Hz, 1H), 3.52 (dd, $J$ = 9.9, 7.0 Hz, 1H), 3.37 (d, $J$ = 3.2 Hz, 1H), 3.24-3.09 (m, 1H), 2.16 (dt, $J$ = 20.4, 10.5 Hz, 1H), 1.93 (dd, $J$ = 12.0, 5.2 Hz, 1H), 1.78 (dd, $J$ = 12.7, 6.8 Hz, 1H), 1.57-1.39 (m, 3H), 1.37-1.08 (m, 4H), 1.00 (s, 6H). $^{13}C$ NMR (75 MHz, DMSO-$d_6$, ppm) $\delta$ 207.59, 160.39, 151.17, 136.08, 129.69, 128.09, 125.04, 125.00, 121.53, 120.06, 114.64, 108.01, 96.32, 74.75, 74.54, 72.04, 63.05, 62.52, 59.62, 54.49, 41.93, 40.99, 38.82, 33.80, 33.19, 30.85, 29.79, 22.11, 20.25. ESI-HRMS calcd for $C_{29}H_{33}ClNO_7^+$ ($[M+H]^+$): 542.1940; found: 542.1945.

*4.2.15 (1S,4aR,5S,6S,6aR,9S,11aS,14R)-1,5,6-trihydroxy-4,4-dimethyl-8-methylene-7-oxododecahydro-1H-6,11b-(epoxymethano)-6a,9-methanocyclohepta[a]naphthalen-14-yl 5-methoxy-1H-indole-2-carboxylate* ***(C3)***

White powder; yield 84%; $[a]_D^{25}$ -9 (c 0.10, $CH_3OH$); $^1H$ NMR (300 MHz, DMSO-$d_6$, ppm) $\delta$ 11.46 (s, 1H), 7.34 (d, $J$ = 8.9 Hz, 1H), 7.09 (d, $J$ = 2.1 Hz, 1H), 6.89 (dd, $J$ = 10.0, 3.4 Hz, 2H), 6.05 (d, $J$ = 10.1 Hz, 2H), 5.94 (d, $J$ = 10.3 Hz, 1H), 5.88 (s, 1H), 5.66 (s, 1H), 4.44 (d, $J$ = 5.0 Hz, 1H), 4.15 (d, $J$ = 10.1 Hz, 1H), 3.87 (d, $J$ = 10.1 Hz, 1H), 3.73 (s, 3H), 3.52 (dd, $J$ = 10.2, 6.8 Hz, 1H), 3.39 (d, $J$ = 4.7 Hz, 1H), 3.16 (d, $J$ = 10.0 Hz, 1H), 2.18 (d, $J$ = 12.4 Hz, 1H), 2.00-1.88 (m, 1H), 1.82-1.71 (m, 1H), 1.50 (dd, $J$ = 26.1, 13.4 Hz, 3H), 1.42-1.12 (m, 4H), 1.00 (s, 6H). $^{13}C$ NMR (75 MHz, DMSO-$d_6$, ppm) $\delta$ 207.73, 160.59, 154.32, 151.16, 133.08, 128.35, 127.40, 120.03, 116.48, 113.87, 108.24, 102.53, 96.33, 74.66, 74.55, 72.05, 63.07, 62.48, 59.65, 55.67, 54.47, 41.93, 40.99, 38.79, 33.79, 33.14, 30.79, 29.79, 22.07, 20.18. ESI-HRMS calcd for $C_{30}H_{36}NO_8^+$ ($[M+H]^+$): 538.2435; found: 538.2434.

*4.2.16 (1S,4aR,5S,6S,6aR,9S,11aS)-1,5,6-trihydroxy-4,4-dimethyl-8-methylene-7-oxododecahydro-1H-6,11b-(epoxymethano)-6a,9-methanocyclohepta[a]naphthalen-14-yl 6-fluoro-1H-indole-2-carboxylate* ***(C4)***

White powder; yield 89%; $[a]_D^{25}$ -71 (c 0.07, $CH_3OH$); $^1H$ NMR (300 MHz, DMSO-$d_6$, ppm) $\delta$ 11.70 (s, 1H), 7.67 (dd, $J$ = 8.8, 5.6 Hz, 1H), 7.16 (d, $J$ = 8.5 Hz, 1H), 6.97 (s, 1H), 6.95-6.87 (m, 1H), 6.07 (d, $J$ = 3.1 Hz, 2H), 5.93 (d, $J$ = 12.5 Hz, 2H), 5.66 (s, 1H), 4.44 (d, $J$ = 4.9 Hz, 1H), 4.13 (dd, $J$ = 12.4, 7.7 Hz, 1H), 3.87 (d, $J$ = 10.1 Hz, 1H), 3.52 (dd, $J$ = 10.1, 6.9 Hz, 1H), 3.18 (d, $J$ = 5.0 Hz, 1H), 2.63-2.53 (m, 1H), 2.15 (dd, $J$ = 20.7, 13.2 Hz, 1H), 1.92 (dd, $J$ = 12.6, 5.1 Hz, 1H), 1.83-1.70 (m, 1H), 1.58-1.44 (m, 3H), 1.35-1.16 (m, 4H), 1.00 (s, 6H). $^{13}C$ NMR (126 MHz, DMSO-$d_6$, ppm) $\delta$ 207.65, 160.37, 151.19, 137.78, 137.60, 129.05, 124.17 (d, $J$ = 10.73 Hz, 1C), 124.00, 120.00, 109.33 ($J$ = 54.75 Hz, 1C), 108.87, 98.40 ($J$ = 25.63 Hz, 1C), 96.29, 74.65, 74.55, 72.05, 63.06, 62.50, 59.64, 54.48, 41.94, 40.99, 38.82, 33.80, 33.17, 30.82, 29.81, 22.09, 20.21. ESI-HRMS calcd for $C_{29}H_{33}FNO_7^+$ ($[M+H]^+$): 526.2236; found: 526.2234.

*4.2.17 (1S,4aR,5S,6S,6aR,9S,11aS,14R)-1,5,6-trihydroxy-4,4-dimethyl-8-methylene-7-oxododecahydro-1H-6,11b-(epoxymethano)-6a,9-methanocyclohepta[a]naphthalen-14-yl 6-chloro-1H-indole-2-carboxylate* ***(C5)***

White powder; yield 74%; $[a]_D^{25}$ -31 (c 0.04, $CH_3OH$); $^1H$ NMR (300 MHz, DMSO-$d_6$, ppm) $\delta$ 11.78 (s, 1H), 7.67 (d, $J$ = 8.6 Hz, 1H), 7.46 (s, 1H), 7.07 (dd, $J$ = 8.6, 1.8 Hz, 1H), 6.96 (s, 1H), 6.08 (s, 2H), 5.92 (t, $J$ = 5.1 Hz, 2H), 5.67 (s, 1H), 4.44 (d, $J$ = 5.0 Hz, 1H), 4.27-4.09 (m, 1H), 3.86 (d, $J$ = 10.2 Hz, 1H), 3.58-3.40 (m, 1H), 3.16 (d, $J$ = 9.4 Hz, 2H), 2.21-2.11 (m, 1H), 1.95 (d, $J$ = 4.1 Hz, 1H), 1.79-1.71 (m, 1H), 1.51-1.45 (d, $J$ = 8.3 Hz, 3H), 1.23-1.16 (d, $J$ = 6.6 Hz, 4H), 1.00 (s, 6H). $^{13}C$ NMR (126 MHz, DMSO-$d_6$, ppm) $\delta$ 207.62, 160.42, 151.18, 137.93, 129.52, 129.27, 125.87, 124.15, 121.13, 120.04, 112.40, 108.67, 96.33, 74.76, 74.56, 72.05, 63.07, 62.52, 59.64, 54.48, 41.93, 41.00, 38.82, 33.81, 33.19, 30.84, 29.81, 22.11, 20.21. ESI-HRMS calcd for $C_{29}H_{33}ClNO_7^+$ ($[M+H]^+$): 542.1940; found: 542.1936.

*4.2.18 (1S,4aR,5S,6S,6aR,9S,11aS,14R)-1,5,6-trihydroxy-4,4-dimethyl-8-methylene-7-oxododecahydro-1H-6,11b-(epoxymethano)-6a,9-methanocyclohepta[a]naphthalen-14-yl 6-bromo-1H-indole-2-carboxylate* ***(C6)***

White powder; yield 64%; $[a]_D^{25}$ -82 (c 0.05, $CH_3OH$); $^1H$ NMR (300 MHz, DMSO-$d_6$, ppm) $\delta$ 11.79 (s, 1H), 7.68-7.57 (m, 2H), 7.18 (dd, $J$ = 8.6, 1.6 Hz, 1H), 6.95 (s, 1H), 6.08 (s, 2H), 5.92 (d, $J$ = 9.3 Hz, 2H), 5.67 (s, 1H), 4.44 (d, $J$ = 5.0 Hz, 1H), 4.15 (d, $J$ = 10.0 Hz, 1H), 3.87 (d, $J$ = 10.2 Hz, 1H), 3.52 (s, 1H), 3.44-3.36 (m, 1H), 3.17 (d, $J$ = 9.3 Hz, 1H), 2.24-2.08 (m, 1H), 1.93 (dd, $J$ = 12.7, 5.1 Hz, 1H), 1.84-1.69 (m, 1H), 1.60-1.42 (m, 3H), 1.37-1.13 (m, 4H), 1.00 (s, 6H). $^{13}C$ NMR (75 MHz, DMSO-$d_6$, ppm) $\delta$ 207.60, 160.41, 151.18, 138.37, 129.12, 126.08, 124.44, 123.61, 120.02, 117.75, 115.43, 108.67, 96.32, 74.77, 74.55, 72.05, 63.07, 62.52, 59.64, 55.37, 41.92, 40.99, 38.83, 33.80, 33.19, 30.84, 29.82, 22.10, 20.24. ESI-HRMS calcd for $C_{29}H_{33}BrNO_7^+$ ($[M+H]^+$): 586.1435; found: 586.1433.

*4.2.19 (1S,4aR,5S,6S,6aR,9S,11aS,14R)-1,5,6-trihydroxy-4,4-dimethyl-8-methylene-7-oxododecahydro-1H-6,11b-(epoxymethano)-6a,9-methanocyclohepta[a]naphthalen-14-yl 6-methoxy-1H-indole-2-carboxylate* ***(C7)***

White powder; yield 87%; $[a]_D^{25}$ -76 (c 0.08, $CH_3OH$); $^1H$ NMR (300 MHz, DMSO-$d_6$, ppm) $\delta$ 11.40 (s, 1H), 7.49 (d, $J$ = 8.8 Hz, 1H), 6.88 (s, 2H), 6.75 – 6.66 (m, 1H), 6.06 (s, 1H), 6.01 (s, 1H), 5.94 (d, $J$ = 10.3 Hz, 1H), 5.86 (s, 1H), 5.65 (s, 1H), 4.43 (d, $J$ = 4.9 Hz, 1H), 4.15 (d, $J$ = 10.0 Hz, 1H), 3.87 (d, $J$ = 9.7 Hz, 1H), 3.77 (s, 3H), 3.52 (dd, $J$ = 10.1, 6.9 Hz, 1H), 3.39 (dd, $J$ = 10.4, 5.4 Hz, 1H), 3.19-3.13 (m, 1H), 2.25-2.12 (m, 1H), 1.92 (d, $J$ = 12.6 Hz, 1H), 1.80-1.71 (m, 1H), 1.52-1.44 (m,3H), 1.30-1.17 (dd, 4H), 1.00 (s, 6H). $^{13}C$ NMR (75 MHz, DMSO-$d_6$, ppm) 207.75, 160.53, 158.29, 151.22, 138.83, 126.94, 123.33, 121.44, 119.95, 112.20, 109.09, 96.34, 94.42, 74.55, 72.09, 72.02, 63.09, 62.47, 59.66, 55.52, 54.44, 41.95, 41.00, 38.83, 33.80, 33.16, 30.79, 29.81, 22.08, 20.19. ESI-HRMS calcd for $C_{30}H_{36}NO_8^+$ ($[M+H]^+$): 538.2435; found: 538.2434.

*4.2.20 (1S,4aR,5S,6S,6aR,9S,11aS)-1,5,6-trihydroxy-4,4-dimethyl-8-methylene-7-oxododecahydro-1H-6,11b-(epoxymethano)-6a,9-methanocyclohepta[a]naphthalen-14-yl 5,6-dimethoxy-1H-indole-2-carboxylate* ***(C8)***

White powder; yield 80%; $[a]_D^{25}$ -85 (c 0.05, $CH_3OH$); $^1H$ NMR (300 MHz, DMSO-$d_6$, ppm) $\delta$ 11.28 (s, 1H), 7.07 (s, 1H), 6.89 (s, 1H), 6.84 (s, 1H), 6.06 (s, 1H), 6.00 (s, 1H), 5.96 (d, $J$ = 10.3 Hz, 1H), 5.84 (s, 1H), 5.65 (s, 1H), 4.44 (d, $J$ = 4.8 Hz, 1H), 4.15 (d, $J$ = 10.2 Hz, 1H), 3.87 (d, $J$ = 10.3 Hz, 1H), 3.78 (s, 3H), 3.73 (s, 3H), 3.56-3.49 (m, 1H), 3.41 (d, $J$ = 6.2 Hz, 1H), 3.16 (d, $J$ = 9.6 Hz, 1H), 2.20-2.14 (d, 1H), 1.96-1.90 (d, 1H), 1.79-1.73 (m, 1H), 1.56-1.45 (m, 3H), 1.37-1.14 (m, 4H), 1.01 (s, 6H). $^{13}C$ NMR (75 MHz, DMSO-$d_6$, ppm) $\delta$ 207.79, 160.41, 151.25, 149.80, 146.03, 133.01, 126.19, 120.05, 108.86, 103.06, 96.36, 94.88, 74.55, 74.51, 72.02, 63.10, 62.45, 59.68, 56.09, 55.83, 55.37, 54.44, 41.96, 40.99, 38.82, 33.81, 33.15, 30.78, 29.82, 22.08, 20.18. ESI-HRMS calcd for $C_{31}H_{38}NO_9^+$ ($[M+H]^+$): 568.2541; found: 568.2540.

*4.2.21 (1S,4aR,5S,6S,6aR,9S,11aS,14R)-1,5,6-trihydroxy-4,4-dimethyl-8-methylene-7-oxododecahydro-1H-6,11b-(epoxymethano)-6a,9-methanocyclohepta[a]naphthalen-14-yl 4,5,6-trimethoxy-1H-indole-2-carboxylate* ***(C9)***

White powder; yield 64%; $[a]_D^{25}$ -100 (c 0.05, $CH_3OH$); $^1H$ NMR (300 MHz, DMSO-$d_6$, ppm) $\delta$ 11.44 (s, 1H), 6.91 (s, 1H), 6.67 (s, 1H), 6.07 (s, 1H), 5.96 (d, $J$ = 12.7 Hz, 2H), 5.92 (s, 1H), 5.66 (s, 1H), 4.43 (d, $J$ = 4.8 Hz, 1H), 4.14 (d, $J$ = 10.4 Hz, 1H), 3.95 (s, 3H), 3.86 (d, $J$ = 10.3 Hz, 1H), 3.80 (s, 3H), 3.69 (s, 3H), 3.52 (dd, $J$ = 10.0, 7.0 Hz, 1H), 3.39 (dd, $J$ = 10.8, 5.1 Hz, 1H), 3.16 (d, $J$ = 5.1 Hz, 1H), 2.17 (dd, $J$ = 14.0, 8.8 Hz, 1H), 1.92 (d, $J$ = 12.3 Hz, 1H), 1.81-1.70 (m, 1H), 1.58-1.44 (m, 3H), 1.36-1.17 (m, 4H), 1.00 (s, 6H). $^{13}C$ NMR (75 MHz, DMSO-$d_6$, ppm) $\delta$ 207.86, 160.38, 153.61, 151.20, 146.13, 135.73, 135.05, 126.25, 119.99, 114.86, 106.77, 96.34, 90.08, 74.67, 74.55, 72.02, 63.09, 62.47, 61.31, 60.88, 59.68, 56.19, 54.43, 41.91, 40.99, 38.80, 33.81, 33.15, 30.80, 29.81, 22.07, 20.16. ESI-HRMS calcd for $C_{32}H_{40}NO_{10}^+$ ($[M+H]^+$): 598.2647; found: 598.2645.

*4.2.22 (1S,4aR,5S,6S,6aR,9S,11aS,14R)-1,5,6-trihydroxy-4,4-dimethyl-8-methylene-7-oxododecahydro-1H-6,11b-(epoxymethano)-6a,9-methanocyclohepta[a]naphthalen-14-yl 1-methyl-1H-indole-3-carboxylate* ***(D1)***

White powder; Yield 81%; $[a]_D^{25}$ -89 (c 0.08, $CH_3OH$); $^1H$ NMR (300 MHz, DMSO-$d_6$, ppm) $\delta$ 7.93 (s, 1H), 7.90 (s, 1H), 7.50 (d, $J$ = 8.1 Hz, 1H), 7.19 (dt, $J$ = 15.0, 7.2 Hz, 2H), 6.06 (d, $J$ = 5.9 Hz, 2H), 6.00 (d, $J$ = 10.2 Hz, 1H), 5.74 (s, 1H), 5.63 (s, 1H), 4.44 (d, $J$ = 5.0 Hz, 1H), 4.16 (d, $J$ = 10.0 Hz, 1H), 3.89 (s, 1H), 3.84 (d, $J$ = 6.2 Hz, 3H), 3.52 (dd, $J$ = 10.0, 6.8 Hz, 1H), 3.45-3.35 (m, 1H), 3.14 (d, $J$ = 9.6 Hz, 1H), 2.29-2.11 (m, 1H), 1.93 (dd, $J$ = 12.6, 4.9 Hz, 1H), 1.83-1.70 (m, 1H), 1.59-1.42 (m, 3H), 1.40-1.11 (m, 4H), 1.01 (s, 6H). $^{13}C$ NMR (75 MHz, DMSO-$d_6$, ppm) $\delta$ 208.14, 163.33, 151.61, 137.37, 136.74, 126.48, 122.74, 121.86, 121.31, 119.71, 111.03, 106.35, 96.40, 74.52, 73.65, 72.07, 63.10, 62.36, 59.75, 54.38, 42.18, 41.01, 38.82, 33.82, 33.46, 33.16, 30.76, 29.84, 22.07, 20.21. ESI-HRMS calcd for $C_{30}H_{36}NO_7^+$ ($[M+H]^+$): 522.2486; found: 522.2483.

*4.2.23 (1S,4aR,5S,6S,6aR,9S,11aS,14R)-1,5,6-trihydroxy-4,4-dimethyl-8-methylene-7-oxododecahydro-1H-6,11b-(epoxymethano)-6a,9-methanocyclohepta[a]naphthalen-14-yl quinoline-6-carboxylate* ***(E)***

White powder; yield 67%; $[a]_D^{25}$ -77 (c 0.13, $CH_3OH$); $^1H$ NMR (300 MHz, DMSO-$d_6$, ppm) $\delta$ 9.02 (s, 1H), 8.55 (d, $J$ = 15.0 Hz, 2H), 8.10 (q, $J$ = 8.9 Hz, 2H), 7.64 (s, 1H), 6.11 (d, $J$ = 12.0 Hz, 2H), 5.98 (s, 1H), 5.76 (s, 1H), 5.67 (s, 1H), 4.18 (d, $J$ = 9.0 Hz, 1H), 3.88 (d, $J$ = 9.2 Hz, 1H), 3.55 (s, 1H), 3.39 (s, 1H), 3.22 (d, $J$ = 9.2 Hz, 1H), 2.69-2.55 (m, 1H), 2.32-2.09 (m, 1H), 1.96 (d, $J$ = 11.9 Hz, 1H), 1.86-1.68 (m, 1H), 1.63-1.40 (m, 3H), 1.35-1.19 (m, 4H), 1.01 (s, 6H). $^{13}C$ NMR (75 MHz, DMSO-$d_6$, ppm) $\delta$ 207.21, 164.05, 150.85, 150.68, 145.96, 140.89, 131.17, 130.28, 129.23, 127.28, 126.63, 122.50, 119.55, 95.89, 75.04, 74.12, 71.57, 62.67, 62.14, 59.29, 53.99, 41.41, 40.55, 38.37, 33.34, 32.68, 30.38, 29.34, 21.61, 19.72. ESI-HRMS calcd for $C_{30}H_{34}NO_7^+$ ($[M+H]^+$): 520.2335; found: 520.2330.

*4.2.24 (1S,4aR,5S,6S,6aR,9S,11aS)-1,5,6-trihydroxy-4,4-dimethyl-8-methylene-7-oxododecahydro-1H-6,11b-(epoxymethano)-6a,9-methanocyclohepta[a]naphthalen-14-yl isoquinoline-1-carboxylate* ***(F)***

White powder; yield 87%; $[a]_D^{25}$ -87 (c 0.11, $CH_3OH$); $^1H$ NMR (300 MHz, DMSO-$d_6$, ppm) $\delta$ 8.69 (d, $J$ = 8.5 Hz, 1H), 8.54 (d, $J$ = 5.5 Hz, 1H), 8.18-8.03 (m, 2H), 7.91-7.84 (m, 1H), 7.82-7.76 (m, 1H), 6.43 (s, 1H), 6.13 (s, 1H), 6.00 (s, 1H), 5.92 (d, $J$ = 9.7 Hz, 1H), 5.65 (s, 1H), 4.47 (d, $J$ = 5.0 Hz, 1H), 4.20 (d, $J$ = 10.2 Hz, 1H), 3.92 (d, $J$ = 10.6 Hz, 1H), 3.55 (dd, $J$ = 9.5, 6.3 Hz, 1H), 3.42 (d, $J$ = 10.1 Hz, 1H), 2.71-2.58 (m, 1H), 2.38-2.23 (m, 1H), 2.05 (dd, $J$ = 12.4, 6.0 Hz, 1H), 1.78-1.68 (m, 1H), 1.60-1.43 (m, 3H), 1.39-1.18 (m, 4H), 1.02 (s, 3H), 0.99 (s, 3H). $^{13}C$ NMR (75 MHz, DMSO-$d_6$, ppm) $\delta$ 207.41, 184.82, 163.82, 150.16, 147.19, 141.19, 136.54, 131.19, 129.29, 127.38, 125.77, 125.02, 119.76, 95.91, 77.34, 73.66, 71.48, 63.06, 62.05, 59.53, 53.77, 40.96, 40.60, 38.34, 33.38, 32.50, 30.39, 29.40, 21.44, 19.45. ESI-HRMS calcd for $C_{30}H_{34}NO_7^+$ ($[M+H]^+$): 520.2335; found: 520.2331.

*4.3 Procedure for the preparation of compound* ***D2***

$CF_3COOH$ (3 mL) was added to a mixture of **9** (36.0 mg) in $CH_2Cl_2$ (15 mL) The reaction was stirred at 0℃for 3 h. After the completion of the reaction, ice water was added, and the mixture was extracted with ethyl acetate three times. The organic phase was washed with brine and dried over anhydrous sodium sulfate. The evaporation of the solvents gave the crude products, which were purified by silica gel column ($CH_2Cl_2$/MetOH, 100:1) to afford **D2**

*4.3.1 (1S,4aR,5S,6S,6aR,9S,11aS,14R)-1,5,6-trihydroxy-4,4-dimethyl-8-methylene-7-oxododecahydro-1H-6,11b-(epoxymethano)-6a,9-methanocyclohepta[a]naphthalen-14-yl 1H-indole-3-carboxylate* ***(D2)***

White powder; yield 34%; $[a]_D^{25}$ -57 (c 0.09, $CH_3OH$); $^1H$ NMR (300 MHz, DMSO-$d_6$, ppm) $\delta$ 12.34 (s, 1H), 8.24 (d, $J$ = 40.7 Hz, 2H), 7.61 (s, 1H), 7.35 (s, 2H), 6.40-5.79 (m, 4H), 5.63 (s, 1H), 4.44 (s, 1H), 4.19 (s, 1H), 3.90 (s, 1H), 3.54 (s, 1H), 3.21 (s, 2H), 2.21 (s, 1H), 1.96 (s, 1H), 1.78 (s, 1H), 1.54 (s, 3H), 1.21 (s, 4H), 1.02 (s, 6H). 13C NMR (126 MHz, DMSO-$d_6$, ppm) $\delta$ 207.96, 163.63, 151.45, 137.07, 127.40, 122.58, 121.09, 119.77, 115.46, 113.23, 111.65, 108.47, 96.36, 74.62, 74.29, 72.05, 63.13, 62.49, 59.73, 54.30, 42.08, 40.99, 38.82, 33.83, 33.15, 29.84, 22.26, 22.09, 20.21. ESI-HRMS calcd for $C_{29}H_{34}NO_7^+$ ($[M+H]^+$): 508.2330; found: 508.2329.

*4.4 Cell lines and cell culture*

3-(4,5-Dimethylthiazol-2-yl)-2,5-diphenyl-2H-tetrazolium bromide (MTT) was purchased from Sigma-Aldrich Co. (St. Louis, MO, USA). The propidium iodide (PI) and Annexin V-FITC apoptosis detection kit were purchased from Invitrogen (Eugene, OR, USA). All human cell lines were used in this study, colorectal cancer cell HCT116, breast cancer cell MCF-7, liver hepatocellular carcinoma cell Bel-7402 and normal liver cell L02 were initially purchased from American Type Culture Collection (ATCC, Manassas, VA, USA). RPMI-1640 media, Dulbecco's modified Eagle's medium (DMEM), and foetal bovine serum (FBS) were provided from Gibco Company (Grand Island, NY, USA). Cell line MCF-7 was cultivated in DMEM containing 10% (v/v) heat-inactivated FBS, 100 units/mL penicillin and 100 μg/mL

streptomycin (Grand Island, NY, USA). Cell lines HCT116, Bel-7402, L02 were cultivated in RPMI 1640 medium containing 10% (v/v) heat-inactivated FBS, 100 units/mL penicillin, and 100 μg/mL streptomycin. The cells were incubated at 37℃under a 5% $CO_2$ and 90% relative humidity (RH) atmosphere.

*4.5 In vitro anticancer activity (MTT assay)*

Cells were plated in 96-well plates at appropriate densities to ensure exponential growth throughout the experimental period ($8\times10^3$ ~ $1\times10^4$ cells per well) and then allowed to adhere for 24 h. Cells were then treated for 48 h with serial concentrations (DMSO, 0.3, 1, 3 and 10 μM) of each compound. 5-fluorouracil (5-Fu) was used as positive control. After 48 h of incubation, 10 μL of MTT solution was added to each well to a final concentration of 2 mg/mL. Plates were then incubated for a further 4 h. After incubation, the MTT solution was removed and 150 μL of DMSO was added to each well for coloration. The plates were shaken vigorously for 10 min at roomtemperature to ensure complete solubilization. The optical density (OD) was read on a microplate reader (ELx 800, BioTek, Highland Park, Winooski, VT, USA) at a wavelength of 492 nm, and the data were subsequently analysed.

*4.6 Colony formation assay*

Exponentially growing determined HCT-116 cells (600 per well) were plated in 6-well plates with the Roswell Park Memorial Institute (RPMI) 1640 culture medium containing with 10% foetal bovine serum (FBS). After 12 h of incubation, the culture medium was removed and replaced fresh medium. Then, the cells were treated with various concentrations of compound **C7** (0.03, 0.06, and 0.12 μM) dissolved in DMSO. Some cells were treated with DMSO only as a negative control. The cells were then incubated for another 7 days. Finally, the cells were fixed with 4% paraformaldehyde for 30 min and stained with 0.1% crystal violet for 15 min at room temperature, after which, the staining was washed with PBS until the colonies were totally cleared. One colony was defined to be an aggregate of > 50 cells. At least three independent experiments were performed for each assay. The numbers of cell colonies

was calculated and analyzed as the ratio of the number of treated samples to untreated samples.

*4.7 Analysis for cell cycle by flow cytometry*

HCT-116 cells were plated in 6-well plates ($5.0\times10^5$ cells per well) and incubated at 37℃ for 24 h. Exponentially growing cells were then incubated with compound **C7** at 0.03 μM, 0.1 μM, 0.3 μM and 1μM. After 24 h, untreated cells (control) or cells treated with compound **C7** were centrifuged at 1000 rpm for 10 min and then fixed in 70% ethanol at -20℃ for at least 24 h. The cells were subsequently resuspended in phosphate-buffered saline (PBS) containing 0.1 mg/mL of RNase A and 5 μg/mL PI. The cellular DNA content for the cell cycle distribution analysis was measured by flow cytometry using a FACSalibur flow cytometer with Cell Quest software (Becton-Dickinson, Franklin Lakes, NJ, USA), plotting at least 30,000 events per sample. The percentage of cells in the G1, S, and G2/M phases of the cell cycle were determined using the ModFit LT version 4.0 software package (Verity Software, Topsham, ME, USA).

*4.8 Analysis of cell morphology by hematoxylin-eosin staining (HE) staining in vitro*

Exponentially growing determined HCT-116 cells ($5 \times 10^6$ per well) were plated in 6-well plates and incubated at 37℃for 24 h. The original culture solution was discarded, and the culture group was added with a culture solution containing different concentrations of **C7** (0.03, 0.1, 0.3, 1.0 μM). Following 24 h of incubation, conventional HE staining was performed, and images were observed and collected under an optical microscope.

*4.9 Analysis for apoptosis by flow cytometry*

Apoptosis was detected using an Apoptosis Detection Kit (Invitrogen, Eugene, OR, USA). In brief, cells were cultured in 6-well plates (5.0×105 cells per well) and incubated at 37℃ for 24 h. Cells with exponential growth were then incubated with compound **C7** at 0.03, 0.1, 0.3, 1.0 and 3.0 μM. Following 24 h of incubation, the

cells were collected, washed twice with PBS and once with 1 × binding buffer for 30 min at room temperature in the dark. Apoptotic cells were enumerated using a FACSCalibur flow cytometer with Cell Quest software (Becton–Dickinson, Franklin Lakes, NJ, USA).

*4.10 Western blot analysis*

HCT-116 cells were cultured with different concentrations of compound **C7** for 24 h. Then, the the floating cells was collected and washed two times with ice cold PBS. The pellet was resuspended in lysis buffer. After the cells were lysed on ice for 20 min, lysates were centrifuged at 12,000 rpm at 4℃for 15 min. Protein concentration was determined by BCA Protein Assay Kit (Beyotime, China) at 570 nm. Equal amounts of protein were resolved using sodium dodecyl sulphate-polyacrylamide gel electrophoresis (SDS-PAGE) (8 ~ 12% acrylamide gels) and transferred to a PVDF Hybond-P membrane (Millipore, Billerica, MS, USA). Membranes were blocked with PBS containing 5% non-fat milk for 1 h at room temperature. Membranes were then incubated with primary antibodies against cyclin A, cyclin B1, Bax, Bcl-2, caspase-9, casase-3, p53, p21, MDM2, β-actin and GAPDH with gentle rotation overnight at 4℃. Membranes were next incubated with fluorescent secondary antibodies for 2 h. Proteins were detected by electrochemiluminescence (Bio-Rad, CA, USA).

*4.11 In vivo antitumor activity.*

Female and male athymic Nu/Nu nude mice (weighing 22 ~ 24 g) were obtained from Vital River (Beijing, China) and housed in specific-pathogen-free conditions in conformity with the Guide for the Care and Use of Laboratory Animals. HCT116 cells ($6 \times 10^6$) suspended in 100 μL saline solution were injected into the right back of mice. After two weeks of tumor transplantation, the mice bearing tumors (an average size of 40 $mm^3$) were divided into 4 groups six animals (half male and half female) at random. The groups with oridonin, **C7** and paclitaxel were administered intraperitoneally (i.p.) 25 mg/kg in a vehicle of 1% DMSO/10% glycero/10% absolute ethanol/79% saline, respectively. The negative control group was treated with the

same vehicle. Treatment were done at a frequency of intraperitoneal injection one dose per day for a total 20 consecutive days. Body weights and tumor volumes were measured every day. On day 21, the tumor-bearing mice were sacrificed, the tumors were excised and weighed. Tumors sizes were determined using caliper measurement and tumors volumes ($mm^3$) were calculated using the standard formula: tumor volume = $(L \times W^2)/2$, Where L is the length and W the width. Ratio of inhibition of tumor (%) = (1 - average tumor weight of treated group/average tumor weight of control group) × 100%.

**Acknowledgements**
This work was supported by the National Natural Science Foundation of China (No. 21662036).

**Abbreviations used**

| | |
|---|---|
| DMF | dimethylformamide |
| DMAP | 4-dimethylaminopyridine |
| EDCI | 1-(3-dimethylaminopropyl)-3-ethylcarbodiimide hydrochloride |
| HCT116 | human colorectal cancer cell line |
| MCF-7 | human breast cancer cell line |
| BEL7402 | human hepatocellular carcinoma cell line |
| MTT | thiazolyl blue tetrazolium bromide |
| 5-Fu | 5-fluorouracil |
| $IC_{50}$ | concentration that inhibits 50% of cell growth. |
| L02 | human normal liver cells |
| SAR | Structure-activity relationship |
| CDK1 | Cyclin-dependent kinase 1 |
| CDK2 | Cyclin-dependent kinase 2 |
| Bcl-2 | B-cell lymphoma 2 |
| Bax | Bcl-2-associated X protein |
| H&E | haematoxylin and eosin |
| p53 | tumor protein p53 |
| p21 | p21Cip1 protein |
| MDM2 | murine double minute chromosome 2 |
| PI | propidium iodide |
| DMEM | Dulbecco's modified Eagle's medium |

FBS foetal bovine serum
OD optical density

**References**

[1] J. Ferlay, I. Soerjomataram, R. Dikshit, S. Eser, C. Mathers, Cancer incidence and mortality worldwide: sources, methods and major patterns in GLOBOCAN 2012, Int. J. Canc. 136 (2015) E359-E386.

[2] D.J. Newman , G.M. Cragg . Natural products as sources of new drugs from 1981 to 2014, J. Nat. Prod. 79 (2016) 629-661.

[3] C.B. Cummins, X.F. Wang, J.M. Xu, B.D. Hughes, Y. Ding, H.Y. Chen, J. Zhou, R.S. Radhakrishnan, Antifibrosis Effect of Novel Oridonin Analog CYD0618 Via Suppression of the NF-kB Pathway, J. Surg. Res. 232 (2018) 283-292.

[4] D.F. Li, H. Wang, Y. Ding, Z.W. Zhang, Z. Zhang, J.B. Dong, H.J. Kim, Q.J. Zhou, J. Zhou, L. Fang, Q. Shen, Targeting the NRF-2/RHOA/ROCK signaling pathway with a novel aziridonin, YD0514, to suppress breast cancer progression and lung metastasis, Cancer Lett. 424 (2018) 97-108.

[5] W. Chen, J.C. Zhou, K.J. Wu, J. Huang, Y. Ding, E.J. Yun, B. Wang, C.Y. Ding, E. Hernandez, J. Santoyo, H.Y. Chen, H. Lin, A. Sagalowsky, D. He, J. Zhou, J.T. Hsieh, Targeting XBP1-mediated $\beta$-catenin expression associated with bladder cancer with newly synthetic Oridonin analogues, Oncotarget. 7 (2016) 56842-56854.

[6] F.J. Bohanon, X.F. Wang, B.M. Graham, C.Y. Ding, Y. Ding, G.L. Radhakrishnan, C. Rastellini, J. Zhou, R.S. Radhakrishnan, Enhanced effects of novel oridonin analog CYD0682 for hepatic fibrosis, J. Surg. Res. 199 (2015) 441-449.

[7] F.J. Bohanon, X.F. Wang, B.M. Graham, A. Prasai, S.J. Vasudevan, C.Y. Ding, Y. Ding, G.L. Radhakrishnan, C. Rastellini, J. Zhou, R.S. Radhakrishnan, Enhanced anti-fibrogenic effects of novel oridonin derivative CYD0692 in hepatic stellate cells, Mol. Cell. Biochem. 410 (2015) 293-300.

[8] S.T. Xu, L.L. Pei, C.Q. Wang, Y.K. Zhang, D.H. Li, HQ. Yao, X.M. Wu, Z.S. Chen, Y.J. Sun, JY. Xu, Novel Hybrids of Natural Oridonin-Bearing Nitrogen Mustards as Potential Anticancer Drug Candidates, ACS Med. Chem. Lett. 5 (2017)

797-802.

[9] D.H. Li, S.T. Xu, H. Cai, LL. Pei, H.Y. Zhang, L. Wang, H.Q. Yao, X.M. Wu, J.Y. Jiang, Y.J. Sun, J.Y. Xu, Enmein-type diterpenoid analogs from natural kaurene-type oridonin: Synthesis and their antitumor biological evaluation, Eur. J. Med. Chem. 64 (2013) 215-221.

[10] D.H. Li, ST. Xu, H. Cai, L.L. Pei, HY. Zhang, L. Wang, X.M. Wu, H.Q. Yao, J.Y. Jiang, Y.J. Sun, J.Y. Xu, Library Construction and Biological Evaluation of Enmein-Type Diterpenoid Analogues as Potential Anticancer Agents, Chem. Med. Chem. 8 (2013) 812-818.

[11] L. Wang, Q. Ren, D.H. Li, H.Q. Yao, Y.H. Zhang, S.T. Yuan, L.Y. Zhang, M.Q. S, J.Y. Xu, Synthesis and Anti-tumor Activity of 14-O-Derivatives of Natural Oridonin, Chin. J. Nat. Medicines. 9 (2011) 194-198.

[12] L. Guo, S.W. Tsang, T.X. Zhang, K.L. Liu, Y.F. Guan, B. Wang, H.D. Sun, H.J. Zhang, M.S. Wong, Efficient Semisynthesis of (−)-Pseudoirroratin A from (−)-Flexicaulin A and Assessment of Their Antitumor Activities, ACS Med. Chem. Lett. 8 (2017) 372-376.

[13] S.T. Xu, H. Yao, S.S. Luo, Y.K. ZHang, D.H. Yang, D.H. Li, G.W. Wang, M. Hu, Y.Y. Qiu, X.M. Wu, H.Q. Yao, W.J. Xie, Z.S. Chen, J.Y. Xu, A Novel Potent Anticancer Compound Optimized from a Natural Oridonin Scaffold Induces Apoptosis and Cell Cycle Arrest through the Mitochondrial Pathway, J. Med. Chem. 60 (2017) 1449-1468.

[14] Y. Ke, J.J. Liang, R.J. Hou, M.M. Li, L.F. Zhao, W. Wang, Y. Liu, H. Xie, R.H. Yang, T.X. Hu, J.Y. Wang, H.M. Liu, Synthesis and biological evaluation of novel Jiyuan Oridonin A-1,2,3-triazole-azole derivatives as antiproliferative agents, Eur. J. Med. Chem. 157 (2018) 1249-1263.

[15] Q.K. Shen, Z.A. Chen, H.J. Zhang, J.L. Li, C.F. Liu, G.H. Gong, Z.S. Quan, Design and synthesis of novel oridonin analogues as potent anticancer agents, J. Enzyme. Inhib. Med. Chem. 33 (2018) 324-333.

[16] Y. Ding, D.F. Li, C.Y. Ding, P.Y. Wang, Z.Q. Liu, E.A. Wold, N. Ye, H.Y. Chen, M.A. White, Q. Shen, J. Zhou, Regio- and Stereospecific Synthesis of

Oridonin D-Ring Aziridinated Analogues for the Treatment of Triple-Negative Breast Cancer via Mediated Irreversible Covalent Warheads, J. Med. Chem. 61 (2018) 2737-2752.

[17] J. Wu, Y. Ding, C.H. Chen, Z.M. Zhou, C.Y. Ding, H.Y. Chen, J. Zhou, C.Chen, A new oridonin analog suppresses triple-negative breast cancer cells and tumor growth via the induction of death receptor 5, Cancer lett. 380 (2016) 393-402.

[18] C.Y. Ding, Y.S Zhang, H.J. Chen, Z.D. Yang, C. Wild, N. Ye, C. D. Ester, A.L. Xiong, M. A. White, Q Shen, and J. Zhou, Oridonin Ring A-Based Diverse Constructions of Enone Functionality: Identification of Novel Dienone Analogues Effective for Highly Aggressive Breast Cancer by Inducing Apoptosis, J. Med. Chem. 56 (2013) 8814-8825.

[19] C.Y. Ding, Y.S Zhang, H.J. Chen, Z.D. Yang, C. Wild, L.L. Chu, H.L. Liu, Q Shen, and J. Zhou, Novel Nitrogen-Enriched Oridonin Analogues with Thiazole-Fused A-Ring: Protecting Group-Free Synthesis, Enhanced Anticancer Profile, and Improved Aqueous Solubility, J. Med. Chem. 56 (2013) 5048-5058.

[20] S.X. Huang, Y. Zhou, J.X. Pu, R.T. Li, X. Li, W.L. Xiao, L.G. Lou, Q.B. Han, L.S. Ding, S.L. Peng, H.D. Sun, Cytotoxic ent-kauranoid derivatives from Isodon rubescens, Tetrahedron 62 (2006) 4941-4947.

[21] S.T. Xu, S.S. Luo, H. Yao, H. Cai, X.M. Miao, F. Wu, D.H. Yang, X.M. Wu, W.J. Xie, H.Q. Yao, Z.S. Chen, J.Y. Xu, Probing the Anticancer Action of Oridonin with Fluorescent Analogues: Visualizing Subcellular Localization to Mitochondria, J. Med. Chem. 59 (2016) 5022-5034.

[22] P.Y. Sun, G.L. Wu, Z.J. Qiu, Y.J. Chen, L-alanine-(14-oridonin) ester trifluoroacetate as well as preparation method and application, Chinese Patent (2014) CN 104017000 A.

[23] V.D. Bock, D. Speijer, H. Hiemstra, J.H. van Maarseveen, 1,2,3-Triazoles as peptide bond isosteres: synthesis and biological evaluation of cyclo-tetrapeptide mimics, Org. Biomol. Chem. 5 (2007) 971-975.

[24] W. Hou, G.J. Zhang, Z. Luo, D. Li, H.Q. Run, B.H. Ruan, L. Su, H.T. Xu, Identification of a diverse synthetic abietane diterpenoid library and insight into

the structure-activity relationships for antibacterial activity, Bioorg. Med. Chem. Lett. 27 (2017) 5382-5386.

[25] K. Lai, P. Yadav, A. Kumar, Synthesis, characterization and antimicrobial activity of 4-((1-benzyl/phenyl-1H-1,2,3-triazol-4-yl)methoxy) benzaldehyde analogues, Med. Chem. Res. 25 (2016) 644-652.

[26] G.C. Brandao, F.C. Rocha Missias, L.M. Arantes, L.F. Soares, K.K. Roy, R.J. Doerksen, A. Braga de Oliveira, G.R. Pereira, Antimalarial naphthoquinones. Synthesis via click chemistry, in vitro activity, docking to PfDHODH and SAR of lapachol-based compounds, Eur. J. Med. Chem. 145 (2018) 1910-205.

[27] M.S. Costa, N. Boechat, E.A. Rangel, C. da Silva Fde, A.M. de Souza, C.R. Rodrigues, H.C. Castro, I.N. Junior, M.C. Lourenco, S.M. Wardell, V.F. Ferreira, Synthesis, tuberculosis inhibitory activity, and SAR study of N-substituted-phenyl-1,2,3-triazole derivatives, Bioorg. Med. Chem. 14 (2006) 8644-8653.

[28] R. De Simone, M.G. Chini, I. Bruno, R. Riccio, D. Mueller, O. Werz, G. Bifulco, Structure-based discovery of inhibitors of microsomal prostaglandin E2 synthase-1, 5-lipoxygenase and 5-lipoxygenase-activating protein: promising hits for the development of new anti-inflammatory agents, J. Med. Chem. 54 (2011) 1565-1575.

[29] F. Naaz, M.C. Preeti Pallavi, S. Shafi, N. Mulakayala, M.S. Yar, H.M. Sampath Kumar, 1,2,3-triazole tethered Indole-3-glyoxamide derivatives as multiple inhibitors of 5-LOX, COX-2 & tubulin: Their anti-proliferative & anti-inflammatory activity, Bioorg. Chem. 81 (2018) 1-20.

[30] M.J. Wu, D.M. Wu, J.B. Chen, J.F. Zhao, L. Gong, Y. X. Gong, Y. Li, X.D. Yang, H.B, Zhang, Synthesis and anti-proliferative activity of allogibberic acid derivatives containing 1,2,3-triazole pharmacophore, Bioorg. Chem. Lett. 28 (2018) 2543-2549.

[31] S. Cho, S. Oh, Y. Um, J.H. Jung, J. Ham, W.S. Shin, S. Lee, Synthesis of 10-substituted triazolyl artemisinins possessing anticancer activity via Huisgen 1,3-dipolar cylcoaddition, Bioorg. Chem. Lett. 19 (2009) 382-385.

[32] Q.K. Shen, C.F. Liu, H.J. Zhang, Y.S. Tian, Z.S. Quan, Design and synthesis of new triazoles linked to xanthotoxin for potent and highly selective anti-gastric cancer agents, Bioorg. Chem. Lett. 27 (2017) 4871-4875.

[33] S. Chekir, M. Debbabi, A. Regazzetti, D. Dargère, O. Laprévote, H.B. Jannet, R. Gharbi, Design, synthesis and biological evaluation of novel 1,2,3-triazole linked coumarinopyrazole conjugates as potent anticholinesterase, anti-5-lipoxygenase, anti-tyrosinase and anti-cancer agents, Bioorg. Chem. 80 (2018) 189-194.

[34] C.Y. Ding, Y.S. Zhang, H.J. Chen, C. Wild, T.Z. Wang, W. Mark A. Q. Shen, J. Zhou, Overcoming synthetic challenges of oridonin A-ring structural diversification: regio- and stereoselective installation of azides and 1,2,3-triazoles at the C-1, C-2, or C-3 position, Org. Lett. 15 (2013) 3718-3721.

[35] S. Lakhdar, M. Westermaier, F. Terrier, R. Goumont, T. Boubaker, A.R. Ofial, H. Mayr, Nucleophilic reactivities of indoles, J. Org. Chem. 71 (2006) 9088-9095

[36] L.B. Diss, S.D. Robinson, Y. Wu, S. Fidalgo, M.S. Yeoman, B.A. Patel, Age-related changes in melatonin release in the murine distal colon, ACS Chem. Neurosci. 4 (2013) 879-887.

[37] A. de Sa, R. Fernando, E.J. Barreiro, M. Fraga, C. Alberto, From nature to drug discovery: the indole scaffold as a ‘privileged structure’, Mini Rev. Med. Chem. 9 (2009) 782-793.

[38] B. Narayana, B. Ashalatha, K.V. Raj, J. Fernandes, B. Sarojini, Synthesis of some new biologically active 1,3,4-oxadiazolyl nitroindoles and a modified Fischer indole synthesis of ethyl nitro indole-2-carboxylates, Bioorg. Med. Chem. 13 (2005) 4638-4644.

[39] W. Hu, Z. Guo, X. Yi, C. Guo, F. Chu, G. Cheng, Discovery of 2-phenyl-3-sulfonylphenyl-indole derivatives as a new class of selective COX-2 inhibitors, Bioorg. Med. Chem. 11 (2003) 5539-5544.

[40] H. Abdel-Gawad, H.A. Mohamed, K.M. Dawood, F.A.-R. Badria, Synthesis and antiviral activity of new indole-based heterocycles, Chem. Pharm. Bull. 58 (2010) 1529-1531.

[41] M.S. Estev ~ ao, L.C. Carvalho, D. Ribeiro, D. Couto, M. Freitas, A. Gomes, L.

Ferreira, E. Fernandes, M.M.B. Marques, Antioxidant activity of unexplored indole derivatives: synthesis and screening, Eur. J. Med. Chem. 45 (2010) 4869-4878.

[42] C. Karaaslan, H. Kadri, T. Coban, S. Suzen, A.D. Westwell, Synthesis and antioxidant properties of substituted 2-phenyl-1H-indoles, Bioorg. Med. Chem. Lett. 23 (2013) 2671-2674.

[43] D. Kumar, N.M. Kumar, B. Noel, K. Shah, A series of 2-arylamino-5-(indolyl)-1, 3, 4-thiadiazoles as potent cytotoxic agents, Eur. J. Med. Chem. 55 (2012) 432-438.

[44] F. Zhang, Y. Zhao, L. Sun, L. Ding, Y. Gu, P. Gong, Synthesis and anti-tumor activity of 2-amino-3-cyano-6-(1*H*-indol-3-yl)-4-phenylpyridine derivatives in vitro, Eur. J. Med. Chem. 46 (2011) 3149-3157.

[45] A. Ahmad, W.A. Sakr, K.M. Rahman, Anticancer properties of indole compounds: mechanism of apoptosis induction and role in chemotherapy, Curr. Drug Targets 11 (2010) 652-666.

[46] Z. Li, M.Y. Luo, B. Cai, H.U. Rashid, M.T. Huang, J. Jiang, L.S. Wang, L.C. Wu, Design, synthesis, biological evaluation and structure-activity relationship of sophoridine derivatives bearing pyrrole or indole scaffold as potential antitumor agents, Eur. J. Med. Chem. 157 (2018) 665-682.

[47] D.L. Boger, D.S. Johnson, CC-1065 and the duocarmycins: understanding their biological function through mechanistic studies, Angew. Chem., Int. Ed. Engl. 35 (1996) 1438−1474.

[48] M. Tercel. H.H. Lee, S.Y. Mehta, J.Y. Tendoung, S. Bai, H.D.S. Liyanage and F.B. Pruijn, Influence of a Basic Side Chain on the Properties of Hypoxia Selective Nitro Analogues of the Duocarmycins: Demonstration of Substantial Anticancer Activity in Combination with Irradiation or Chemotherapy, J. Med. Chem. 60 (2017) 5834−5856.

[49] Z.C. Dai, Y.F. Chen, M. Zhang, S.K. Li, T.T. Yang, L. Shen, J.X. Wang, S.S. Qian, H.L. Zhu, Y.H. Ye, Synthesis and Antifungal Activity of 1,2,3-Triazole Phenylhydrazone Derivatives, Org. Biomol. Chem. 13 (2015) 477-486.

[50] Z. Jia, Q. Zhu,'Click' assembly of selective inhibitors for MAO-A, Bioorg. Med. Chem. Lett. 20 (2010) 622-6225.

[51] F. Zhang, Y.F. Zhao, L. Sun, L. Ding, Y.C. Gu, P. Gong, Synthesis and anti-tumor activity of 2-amino-3-cyano-6-(1H-indol-3-yl)-4-phenylpyridine derivatives *in vitro*, Eur. J. Med. Chem. 46 (2011) 3149-3157.

[52] J.R. Davies, P.D. Kane, C.J. Moody and A.M.Z. Slawin, Control of Competing N-H Insertion and Wolff Rearrangement in Dirhodium(II)-Catalyzed Reactions of 3-Indolyl Diazoketoesters. Synthesis of a Potential Precursor to the Marine 5-(3-Indolyl)oxazole Martefragin A, J. Org. Chem. 70 (2005) 5840-5851.

[53] H.S.G. Beckmann, F. Nie, C.E. Hagerman, H. Johansson, Y.S. Tan, D. Wilcke and D.R. Spring, A strategy for the diversity-oriented synthesis of macrocyclic scaffolds using multidimensional coupling, Nature Chem. 5 (2013) 861-867.

[54] D.H. Li, L. Wang, H. Cai, Y.H. Zhang and J.Y. Xu, Synthesis and Biological Evaluation of Novel Furozan-Based Nitric Oxide-Releasing Derivatives of Oridonin as Potential Anti-Tumor Agents, Molecules 17 (2012) 7556-7568.

[55] D.D. Luo, K. Peng, J.Y. Yang, P. Piyachaturawat, W. Saengsawang, L. Ao, W.Z. Zhao, Y. Tang and S.B. Wan, Structural modification of oridonin via DAST induced rearrangement, RSC Adv. 8 (2018) 29548-29554.

[56] G.K. Dy, A.A. Adjei, Understanding, recognizing, and managing toxicities of targeted anticancer theratpies, Ca-Cancer J. Clin. 63 (2013) 249-279.

[57] K. F. Lei, Z.M. Wu, C.H. Huang, Impedimetric quantification of the formation process and the chemosensitivity of cancer cell colonies suspended in 3D environment, Biosens. Bioelectron, 74 (2015) 878-885.

[58] G. Joshi, P.K. Singh, A. Negi, A. Rana, S. Singh, R. Kumar, Growth factors mediated cell signalling in prostate cancer progression: implications in discovery of anti-prostate cancer agents, Chem. Biol. Interact. 240 (2015) 120-133.

[59] A. Marais, Z. Ji, E.S. Child, E. Krause, D.J. Mann, A.D. Sharrocks, Cell cycle-dependent regulation of the forkhead transcription factor FOXK2 by CDK$ cyclin complexes, J. Biol. Chem. 285 (2010) 35728-35739.

[60] S. Kalra, G. Joshi, A. Munshi, R. Kumar, Structural insights of cyclin dependent

kinases: Implications in design of selective inhibitors, Eur. J. Med. Chem. 142 (2017) 424-458.

[61] Y. Liu, J.H. Li, H. Xu, Y.W. Zhang, Y.L. Liu, Y.H. Liu, Mitochondria-mediated tumstatin peptide-induced HepG2 cell apoptosis, Int. J. Mol. Med. 24 (2009) 653-659.

[62] M.S. Ola, M. Nawaz, H. Ahsan, Role of Bcl-2 family proteins and caspases in theregulation of apoptosis, Mol. Cell. Biochem. 351 (2011) 41-58.

[63] S. Niazi, M. Purohit and J.H. Niazi, Role of p53 circuitry in tumorigenesis: a brief review, Eur. J. Med. Chem. 158 (2018) 7-24.

[64] Y. Ding, C.Y. Ding, N. Ye, Z.Q. Liu, E.A. Wold, H.Y. Chen, C. Wild, Q. Shen, J. Zhou, Discovery and development of natural product oridonin-inspired anticancer agents, Eur. J. Med. Chem. 122 (2016) 102-117.

[65] J.M. Xu, E.A. Wold, Y. Ding, Q. Shen, J. Zhou, Therapeutic potential of oridonin and its analogs: from anticancer and antiinflammation to neuroprotection, Molecules 23 (2018) 474/1-474/16.

[66] Y. Cheng, F. Qiu, Y.C. Ye, S. Tashiro, S. Onodera and T. Ikejima, Oridonin induces G2/M arrest and apoptosis via activating ERK-P53 apoptotic pathway and inhibiting PTK-Ras-Raf-JNK survival pathway in murine fibrosarcoma L929 cells, Arch. Biochem. Biophys. 490 (2009) 70-75.

[67] A. Gollner, D. Rudolph, H. Arnhof, M. Bauer, S.M. Blake, G. Boehmelt, X.L. Cockroft, G. Dahmann, P. Ettmayer, T. Gerstberger, J. Karolyi-Oezguer, D. Kessler, C. Kofink, J. Ramharter, J. Rinnenthal, A. Savchenko, R. Schnitzer, H. Weinstabl, U. Weyer-Czernilofsky, T. Wunberg, D.B. McConnell, Discovery of Novel Spiro[3*H*-indole-3,2-pyrrolidin]-2(1*H*)-one Compounds as Chemically Stable and Orally Active Inhibitors of the MDM2-p53 Interaction, J. Med. Chem. 59 (2016) 10147-10162.

[68] H.K. Koblish, S. Zhao, C.F. Franks, R.R. Donatelli, R.M. Tominovich, L. V LaFrance, K. Leonard, J.M. Gushue, D.J. Parks, R.R. Calvo, K.L. Milkiewicz, J.J. Marugán, P. Raboisson, M.D. Cummings, B.L. Grasberger, D.L. Johnson, T. Lu, C.J. Molloy, A.C. Maroney, Benzodiazepinedione inhibitors of the

Hdm2:p53 complex suppress human tumor cell proliferation in vitro and sensitize tumors to doxorubicin in vivo, Mol. Cancer Ther. 5 (2006) 160-169

[69] Z. Yu, C. Zhuang, Y. Wu, Z. Guo, J. Li, G. Dong, J. Yao, C. Sheng, Z. Miao, W. Zhang, Design, synthesis and biological evaluation of sulfamide and triazole benzodiazepines as novel p53-MDM2 inhibitors, Int. J. Mol. Sci. 15 (2014) 15741-15753.

[70] A. Vaupel, G. Bold, A.D. Pover, T.S. Valat, J.H. Lisztwan, J. Kallen, K. Masuya, P. Furet, Tetra-substituted imidazoles as a new class of inhibitors of the p53-MDM2 interaction, Bioorg. Med. Chem. Lett. 24 (2014) 2110-2114.

**Table 1.** Antiproliferative efficacy of oridonin derivatives of compounds **A1-9**, **B1-3**, **C1-9**, **D1-2**, **E**, **F** in three human cancer cell lines[a].

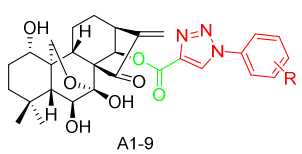
A1-9

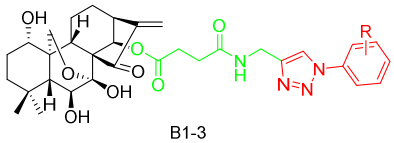
B1-3

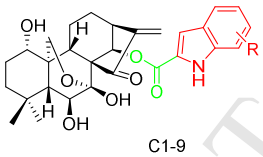
C1-9

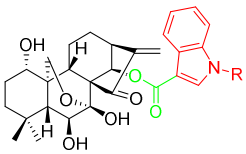
D1-2

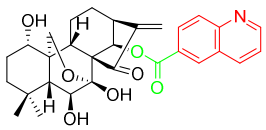
E

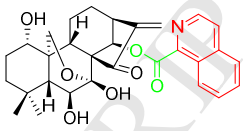
F

| Comound | R | $IC_{50}$ values ($\mu$M)[b] | | |
|---|---|---|---|---|
| | | HCT116 | MCF-7 | Bel7402 |
| **A1** | 4-H | 3.86 ± 1.01 | 6.24 ± 0.78 | 6.11 ± 0.99 |
| **A2** | 2-F | 4.95 ± 1.12 | 5.66 ± 1.35 | 9.02 ± 1.14 |
| **A3** | 4-F | 2.52 ± 0.64 | 5.73 ± 2.34 | 5.58 ± 1.34 |
| **A4** | 4-Cl | 3.52 ± 0.51 | 4.79 ± 0.82 | 6.47 ± 1.07 |
| **A5** | 4-$CH_3$ | 3.51 ± 0.92 | 3.01 ± 0.71 | 7.85 ± 1.20 |
| **A6** | 4-$OCH_3$ | 1.94 ± 0.35 | 3.83 ± 0.31 | 6.42 ± 1.11 |
| **A7** | 3,4-$OCH_3$ | 2.89 ± 0.36 | 5.91 ± 1.03 | 5.52 ± 0.97 |
| **A8** | 3,4,5-$OCH_3$ | 3.67 ± 1.03 | 6.74 ± 0.99 | 6.89 ± 1.09 |
| **A9** | 4-$NO_2$ | 5.60 ± 1.55 | 4.34 ± 0.33 | 8.84 ± 1.87 |
| **B1** | 4-H | 6.89 ± 1.02 | 6.81 ± 1.23 | 12.68 ± 2.13 |
| **B2** | 4-Cl | 7.31 ± 0.89 | 14.99 ± 2.67 | 11.07 ± 2.89 |
| **B3** | 4-$OCH_3$ | 5.05 ±1.03 | 12.81 ± 1.34 | 9.67 ± 1.21 |
| **C1** | 5-H | 2.64 ± 0.24 | 0.78 ± 0.14 | 3.12 ± 0.69 |
| **C2** | 5-Cl | 1.64 ± 0.32 | 2.45 ± 0.38 | 2.10 ± 0.19 |
| **C3** | 5-$OCH_3$ | 0.81 ± 0.12 | 0.39 ± 0.09 | 0.83 ± 0.15 |
| **C4** | 6-F | 0.29 ± 0.08 | 1.25 ± 0.27 | 3.03 ± 0.95 |
| **C5** | 6-Cl | 0.82 ± 0.14 | 1.83 ± 0.34 | 2.74 ± 0.88 |
| **C6** | 6-Br | 0.68 ± 0.10 | 0.83 ± 0.04 | 1.73 ± 0.27 |
| **C7** | 6-$OCH_3$ | 0.16 ± 0.04 | 1.52 ± 0.39 | 2.18 ± 0.19 |
| **C8** | 5,6-$OCH_3$ | 1.67 ± 0.21 | 0.94 ± 0.13 | 2.39 ± 0.37 |
| **C9** | 4,5,6-$OCH_3$ | 0.55 ± 0.12 | 1.20 ± 0.28 | 1.97 ± 0.42 |
| **D1** | -$CH_3$ | 1.17 ± 0.31 | 0.95 ± 0.12 | 3.95 ± 0.19 |
| **D2** | -H | 2.73 ± 0.63 | 3.81 ± 0.78 | 5.31 ± 0.96 |
| **E** | - | 2.51 ± 0.16 | 0.41 ± 0.09 | 2.54 ± 0.66 |
| **F** | - | 2.07 ± 0.38 | 0.89 ± 0.17 | 2.30 ± 0.39 |
| **Oridonin** | - | 6.84 ± 0.98 | 17.56 ± 3.65 | 9.59 ± 1.19 |
| **5-Fu** | - | 24.80 ± 2.08 | 16.28 ± 1.78 | 21.3 ± 2.43 |

[a]MTT methods; cells were incubated with indicated compounds for 48 h (means ± SD, n = 3).
[b]$IC_{50}$ : concentration that inhibits 50% of cell growth.

**Table 2.** *In vitro* cytotoxic of compounds **C1**, **C3-8**, **D1**, **E** and **F** against normal cell line (L02).

| Comound | LO2 ($IC_{50}$, μM)[a] | Selectivity index [b] | | |
|---|---|---|---|---|
| | | HCT-116 | MCF-7 | Bel-7402 |
| **C1** | 4.22 ± 0.78 | 1.60 | 5.41 | 1.35 |
| **C3** | 3.72 ± 0.92 | 4.59 | 9.54 | 4.48 |
| **C4** | 4.08 ± 1.03 | 14.07 | 3.26 | 1.35 |
| **C5** | 3.51 ± 0.58 | 4.28 | 1.92 | 1.28 |
| **C6** | 2.74 ± 0.32 | 4.03 | 3.30 | 1.58 |
| **C7** | 3.78 ± 0.89 | 23.63 | 2.49 | 1.73 |
| **C8** | 3.17 ± 0.66 | 1.90 | 3.37 | 1.33 |
| **C9** | 2.58 ± 0.51 | 4.69 | 2.15 | 1.31 |
| **D1** | 4.19 ± 0.25 | 3.58 | 4.41 | 1.06 |
| **E** | 1.25 ± 0.12 | 0.50 | 3.05 | 0.49 |
| **F** | 1.99 ± 0.22 | 0.96 | 2.24 | 0.87 |
| **Oridonin** | 6.97 ± 0.98 | 1.02 | 0.40 | 0.73 |
| **5-Fu** | 19.12 ± 1.01 | 0.65 | 1.17 | 0.90 |

[a] $IC_{50}$ : concentration that inhibits 50% of cell growth.
[b] SI: selective index ($IC_{50}$ on normal cells/$IC_{50}$ on tumour cells).

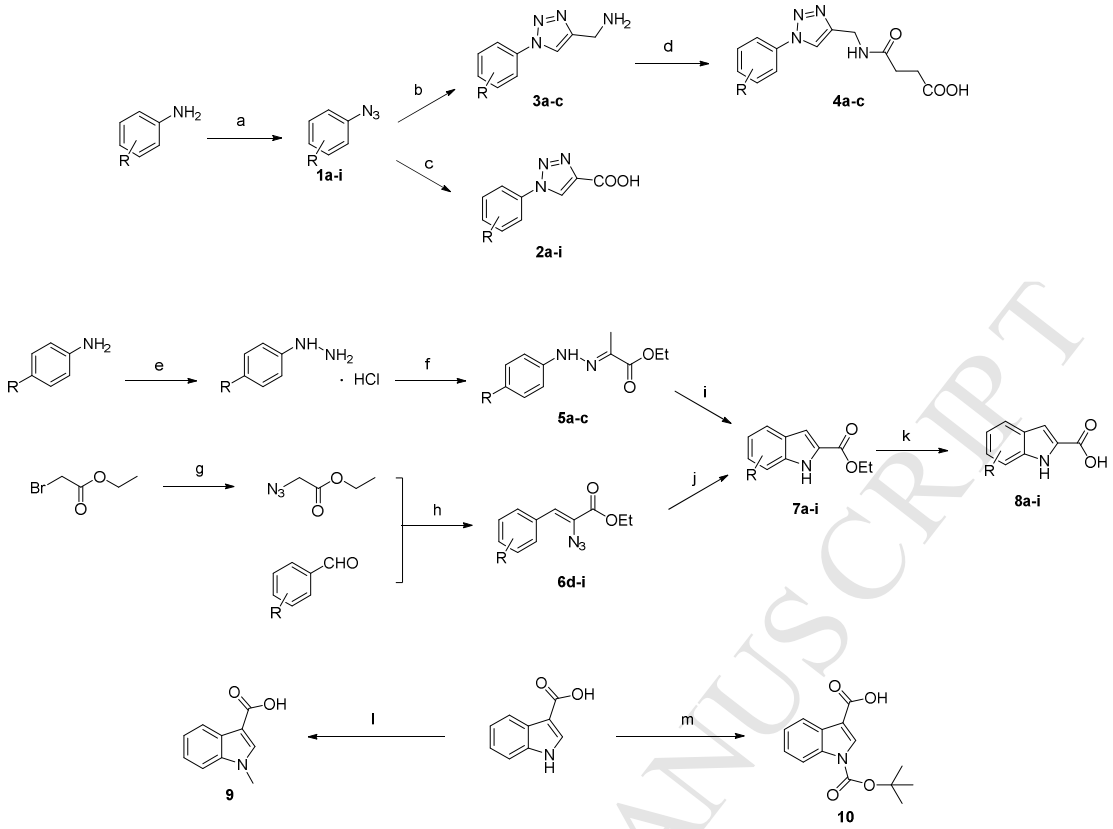


**Scheme 1.** Reagents and conditions: (a) (i) HCl, $NaNO_2$, $H_2O$, 0-5 □, 30 min; (ii) $NaN_3$, $H_2O$, 0-5□, 2-4 h; (b) propiolic acid, Na ascorbate, $CuSO_4.5H_2O$, $H_20$, *t*-BuOH/$H_2O$, 25□, overnight; (c) propynylamine, $CuSO_4 \cdot 5H_2O$, sodium ascorbate, *t*-BuOH/$H_2O$ (1:1), 80 □, 19 h; (d) succinic anhydride, $CH_2Cl_2$, r.t.. (e) (i) $NaNO_2$, HCl, $H_2O$, 1 h; (ii) $NaHSO_3$ , NaOH, $H_2O$, 80 □, 1 h; (iii) HCl, $H_2O$, reflux, 3 h; (f) Pyruvate, AcOH, EtOH, reflux, 3-5 h; (g) $NaN_3$ , MeCN, 63 □, 4 h; (h) different substituted benzaldehyde, EtONa, EtOH, 0□, 4-8 h; (i) PPA, 100 □, 4 h; (j) xylene, reflux, 3-5 h; (k) NaOH, EtOH, reflux, 3 h, HCl; (l) $CH_3I$, KOH, DMF, r.t., 2 h; (m) Di-tert-butyl dicarbonate, DMAP, $CH_2Cl_2$, r.t., overnight.

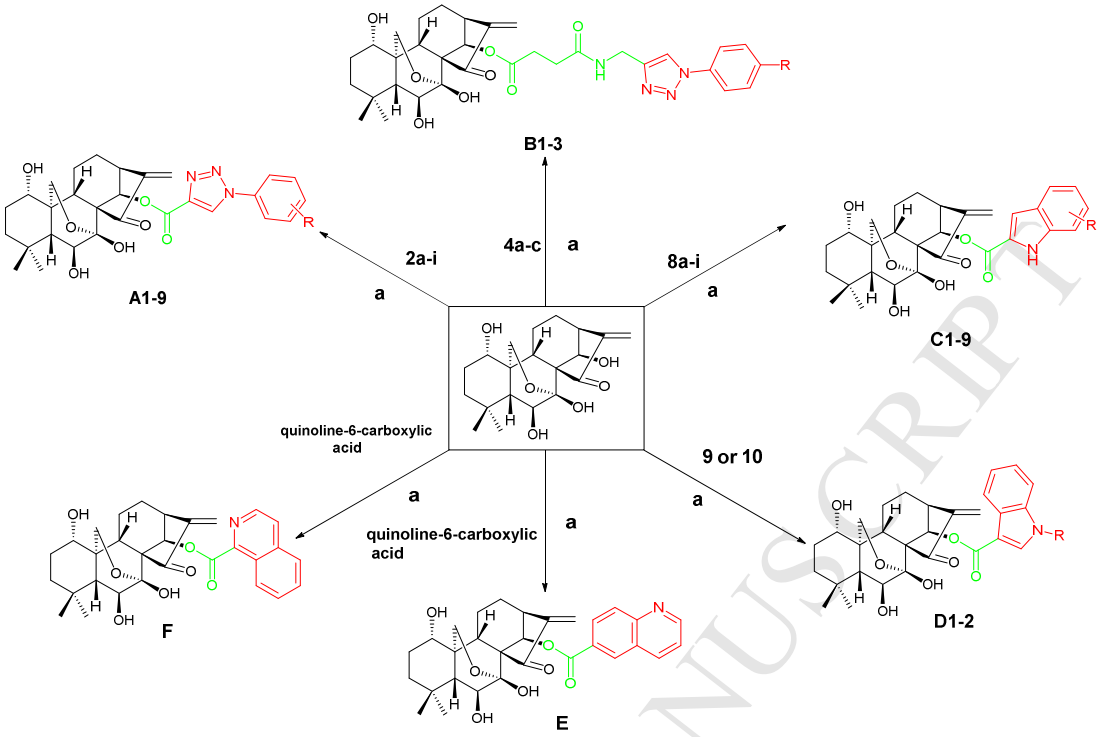


| | | | | |
|---|---|---|---|---|
| **A1**: R = H | **A2**: R = 2-F | **A3**: R = 4-F | **A4**: R = 4-Cl | **A5**: R = 4-$CH_3$ |
| **A6**: R = 4-$OCH_3$ | **A7**: R = 3,4-$OCH_3$ | **A8**: R = 3,4,5-$OCH_3$ | **A9**: R = 4-$NO_2$ | |
| **B1**: R= 4-H | **B2**: R = 4-Cl | **B3**: R = 4-$0CH_3$ | | |
| **C1**: R = H | **C2**: R = 5-Cl | **C3**: R = 5-$OCH_3$ | **C4**: R = 6-F | **C5**: R = 6-Cl |
| **C6**: R = 6-Br | **C7**: R = 6-$OCH_3$ | **C8**: R = 5,6-$OCH_3$ | **C9**: R = 4,5,6-$OCH_3$ | |
| **D1**: R = $CH_3$ | **D3**: R = Boc | **D2**: R= H | | |

b

**Scheme 2.** Reagents and conditions: (a) oridonin, EDCI, DMAP, dry $CH_2Cl_2$, 0 □, 2-8 h. (b) $CF_3COOH$, $CH_2Cl_2$, 0 □, 2 h.

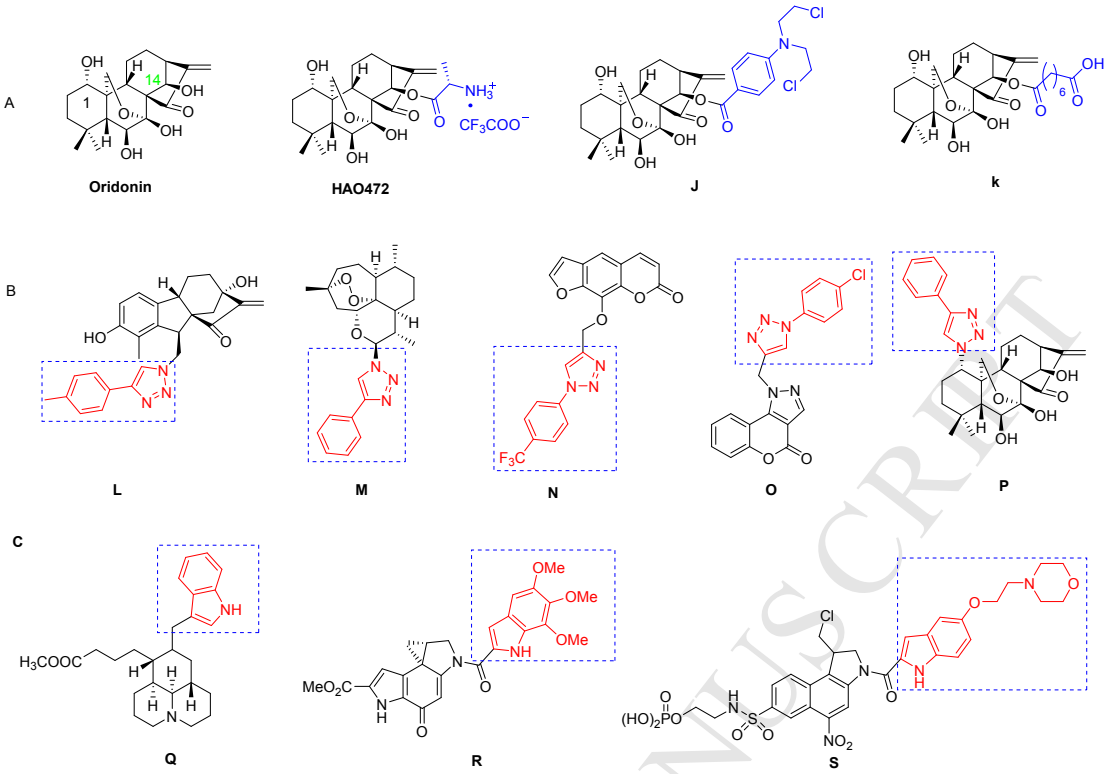


**Figure 1.** (A) Structures of oridonin and its C-14 derivatives; (B) Structures of natural product derivatives containing phenyl 1,2,3-triazole; (C) Structures of natural product derivatives containing indole.

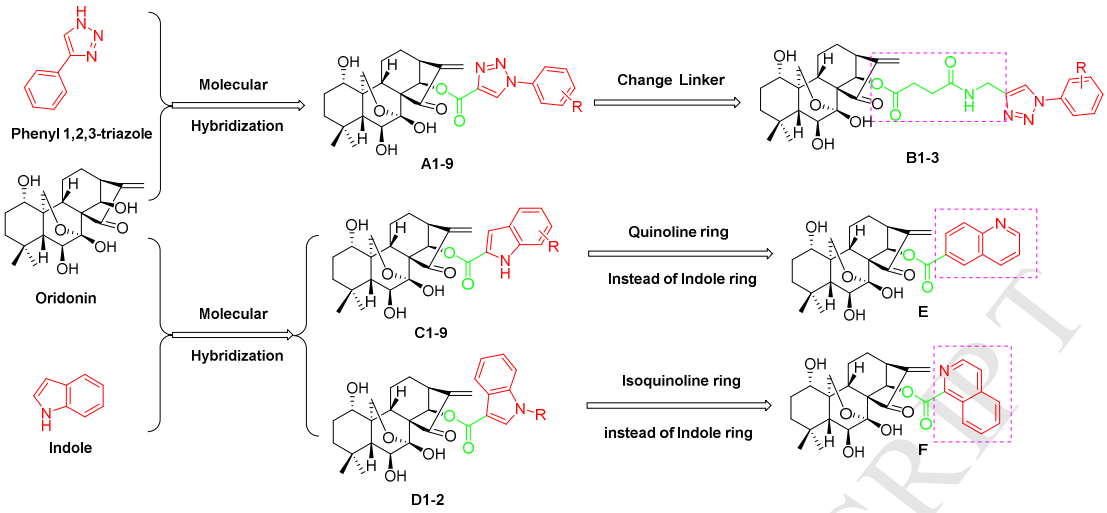


**Figure 2.** Designing oridonin derivatives containing a nitrogen-containing heterocycle to achieve potential anti-proliferative activity.

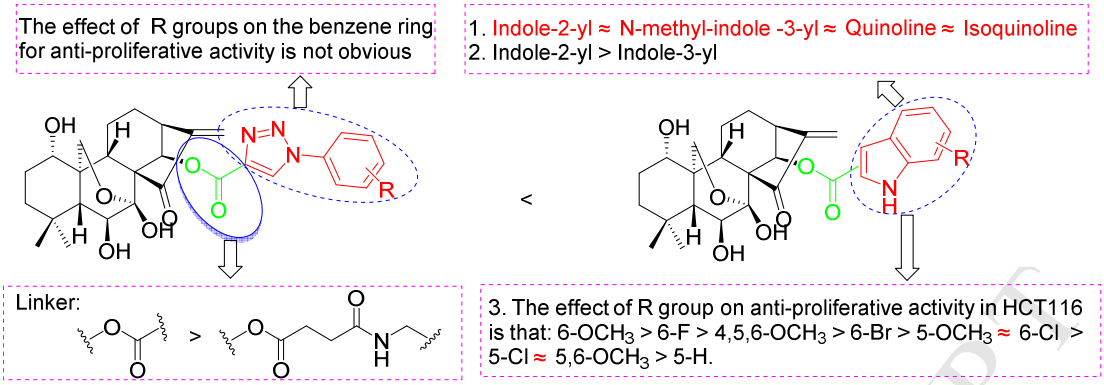


**Figure 3.** Structure activity relationship (SAR) of 14-substituted oridonins.

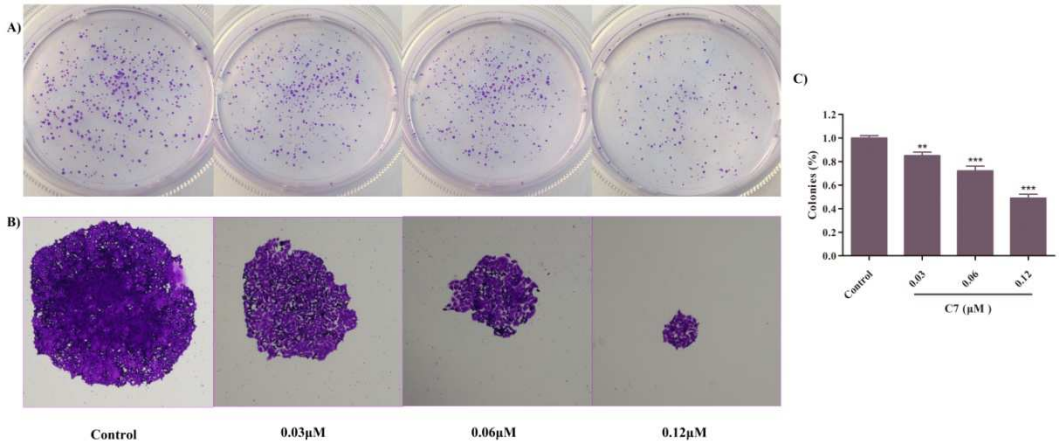


**Figure 4.** Colony formation of HCT116 cells inhibited by compound **C7**. (A) HCT116 cells were incubated with varying concentrations of **C7** (0, 0.03, 0.06, 0.12 $\mu$M) and stained with crystal violet. (B) The micrographic differences between the colonies. Images were taken of stained single colonies observed under a microscope. (C) Bar chart showing the decreased proportion of the colonies after incubation with **C7**. One colony was defined to be an aggregate of > 50 cells. Data are shown as the mean ± SD of three independent experiments, **p < 0.01 and ***p < 0.001 vs control group (untreated cells).

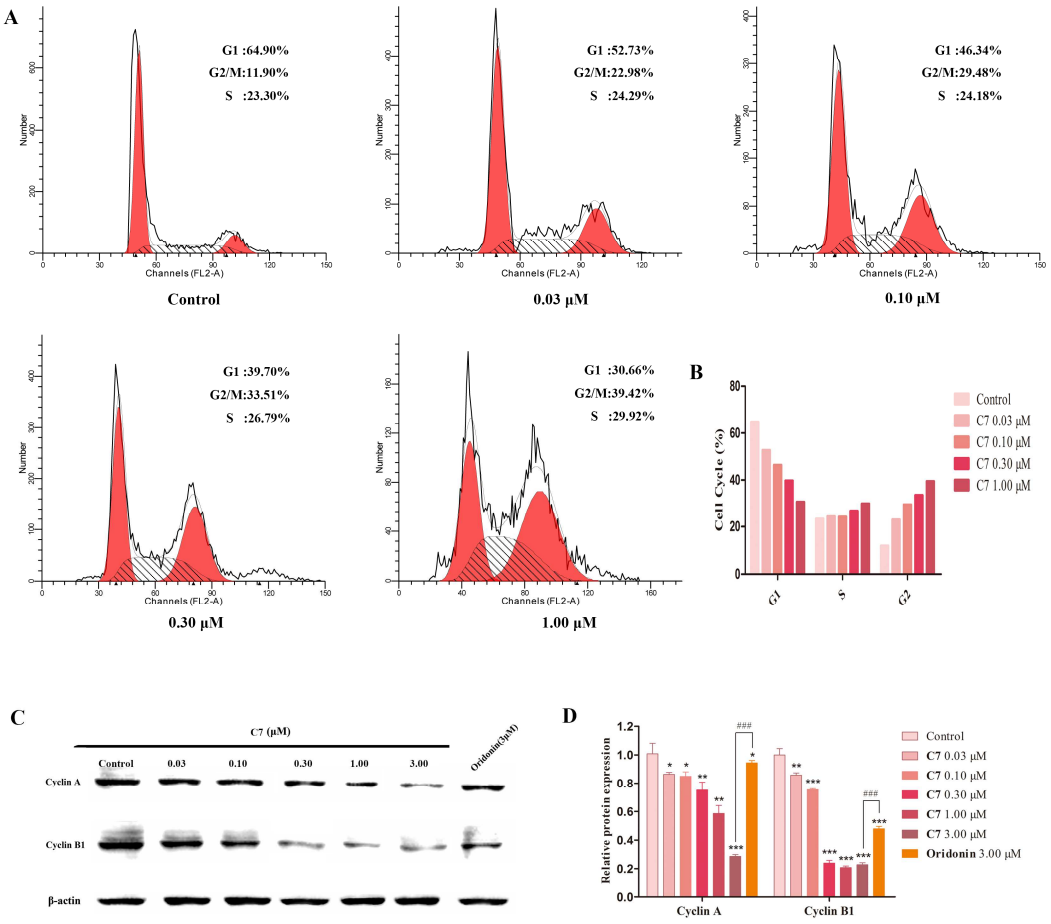


**Figure 5.** Compound **C7** induced S and G2/M arrest in HCT116 cancer cells. (A) HCT116 cells were incubated varying concentrations of **C7** (0, 0.03, 0.10, 0.3, 1.00 $\mu$M). (B) Histograms display the percentage of cell cycle distribution. (C) Western blotting analysis on the effect of **C7** on the G2/M regulatory proteins. The cells were harvested and lysed for the detection of cyclin A and cyclin B1. (D) Histograms display the density ratio of cyclin A and cyclin B1 to $\beta$-actin. Data are represented as mean $\pm$ SD of three independent experiments. *p < 0.05, **p < 0.01, and ***p < 0.001 compared with Control group; $^{###}$p < 0.001 compared with Oridonin group.

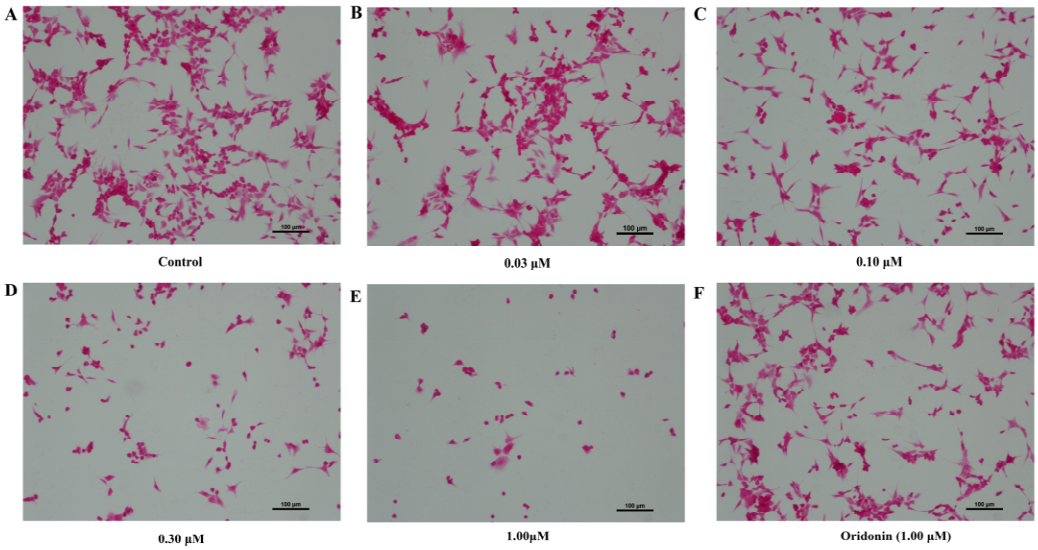


**Figure 6.** Cell morphological alterations and nuclear changes associated with HCT116 cells after incubation with varying concentrations **C7** (0, 0.03, 0.1, 0.3, 1.0 $\mu$M) and Oridonin (1.00 $\mu$M) for 24h were assessed by staining with H&E and visualized by microscopy.

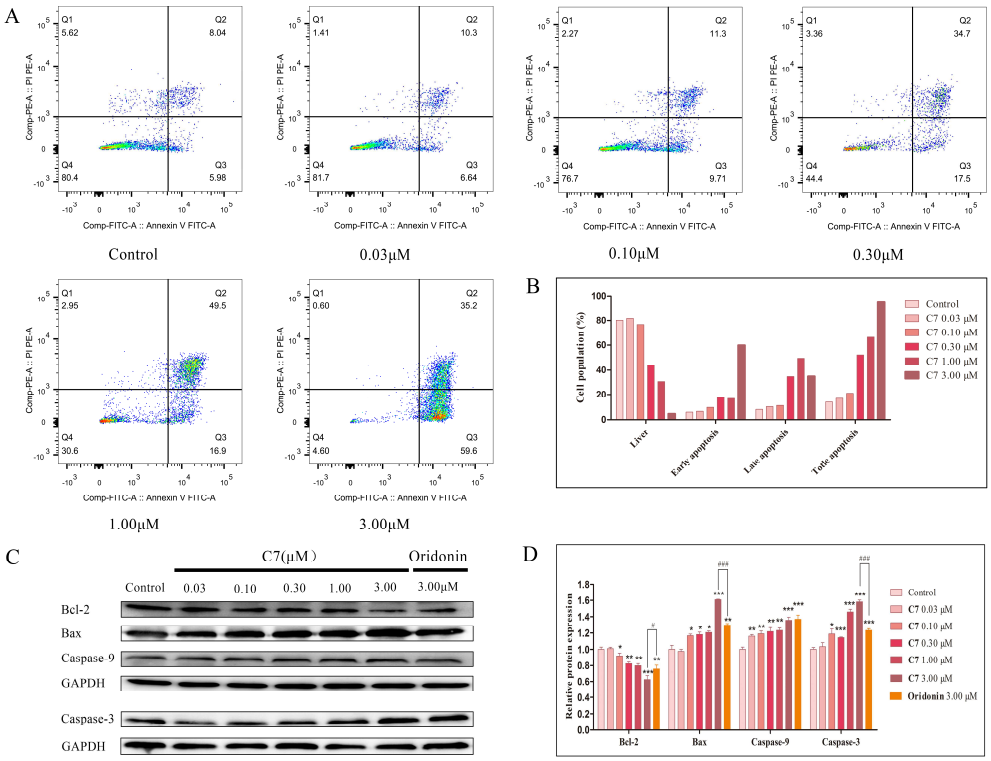


**Figure 7.** Compound **C7** induced apoptosis of HCT116 cells. (A) HCT116 cells were incubated varying concentrations of **C7** (0, 0.03, 0.10, 0.30, 1.00, 3.00 $\mu$M). (B) Histograms display the percentage of cell apoptosis distribution. (C) Western blotting analysis on the effect of **C7** on the cell apoptosis regulatory proteins. The cells were harvested and lysed for the detection of Bcl-2, Bax, Casase-9, and Casase-3. (f) Histograms display the density ratio of regulatory proteins to GAPDH. Data are represented as mean $\pm$ SD of three independent experiments. *p < 0.05, **p < 0.01, and ***p < 0.001 compared with Control group; $^{\#}$p < 0.05, and $^{\#\#\#}$p < 0.001 compared with Oridonin group.

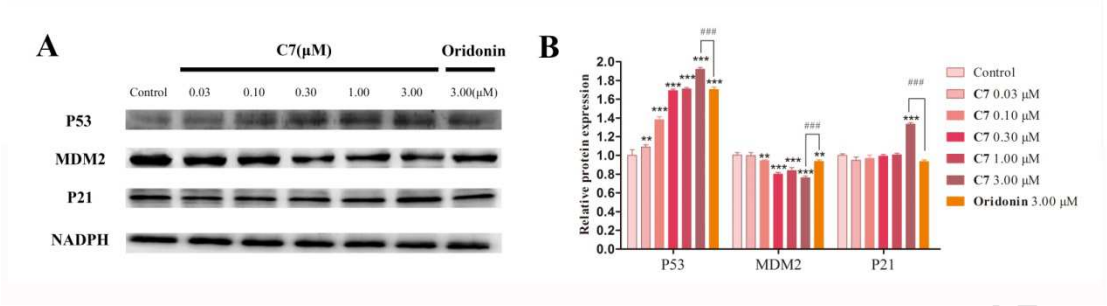


**Figure 8. (**A**)** Western blotting analysis on the effect of **C7** on the cell p53 regulatory proteins. The cells were harvested and lysed for the detection of p53, MDM2, and p21. (B) Histograms display the density ratio of regulatory proteins to GAPDH. Data are represented as mean ± SD of three independent experiments. *$p < 0.05$, **$p < 0.01$, and ***$p < 0.001$ compared with Control group; $^{###}p < 0.001$ compared with Oridonin group.

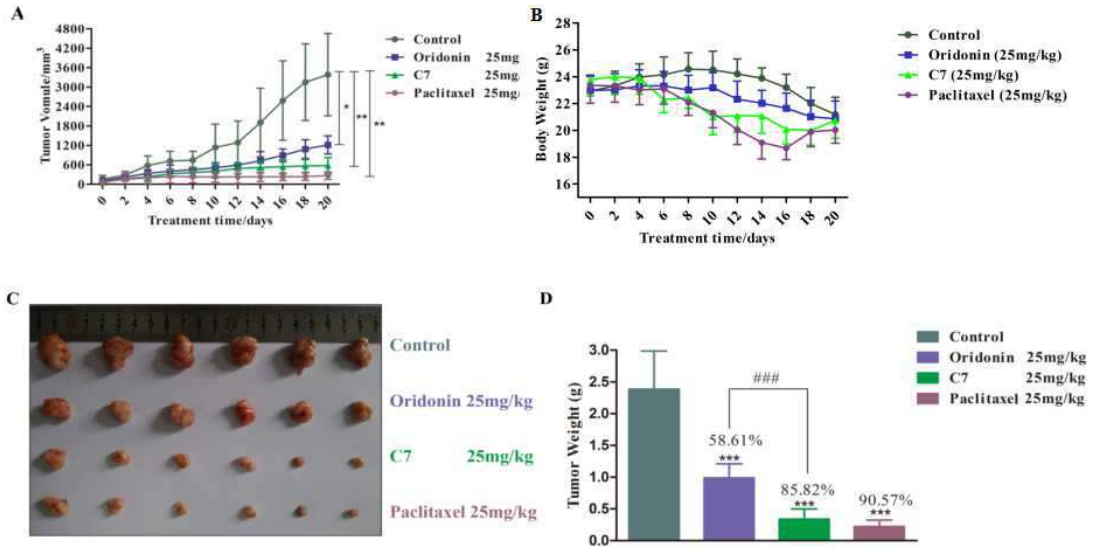


**Figure 9.** Compound **C7** inhibits colon cancer xenograft growth *in vivo*. (A) The mice were randomly divided into four groups with 6 mice in each group and treated intraperitoneally with control, oridonin (25 mg/kg), **C7** (25 mg/kg), and paclitaxel (25 mg/kg) every day for 20 days and the figure showed the average measured tumor volumes, *$p < 0.05$, and **$p < 0.01$ compared with Control group; (B) Body weight of mice before dissection; (C) The resulting tumors were excised from the animals after treatment; (D) Histograms display the changes of tumor weight, *$p < 0.05$, **$p < 0.01$, and ***$p < 0.001$ compared with Control group; $^{###}p < 0.001$ compared with Oridonin group.

**Highlights:**

- Novel oridonin derivatives have been designed, synthesized, and evaluated as anticancer agents against three cancer cell lines.
- Compound **C7** was 43-fold more efficacious than oridonin in HCT116 cancer cells.
- p53-MDM2 Pathway may be involved in **C7** induced the arrest of G2/M phase and apoptosis in HCT116 cancer cells.
- **C7** significantly inhibited tumor growth and had no observable toxic effect *in vivo*.